Multipole Expansion for Transient Electric and Magnetic Fields in an Internally Excited Spherical Cavity Containing Dampers of Finite Thickness with Distributed Electrical Properties

B. P. Curry
ARO, Inc.

October 1981

Final Report for Period October 1, 1979 – September 30, 1980

ARNOLD ENGINEERING DEVELOPMENT CENTER
ARNOLD AIR FORCE STATION, TENNESSEE
AIR FORCE SYSTEMS COMMAND
UNITED STATES AIR FORCE

NOTICES

When U. S. Government drawings, specifications, or other data are used for any purpose other than a definitely related Government procurement operation, the Government thereby incurs no responsibility nor any obligation whatsoever, and the fact that the Government may have formulated, furnished, or in any way supplied the said drawings, specifications, or other data, is not to be regarded by implication or otherwise, or in any manner licensing the holder or any other person or corporation, or conveying any rights or permission to manufacture, use, or sell any patented invention that may in any way be related thereto.

Qualified users may obtain copies of this report from the Defense Technical Information Center.

References to named commercial products in this report are not to be considered in any sense as an indorsement of the product by the United States Air Force or the Government.

This report has been reviewed by the Office of Public Affairs (PA) and is releasable to the National Technical Information Service (NTIS). At NTIS, it will be available to the general public, including foreign nations.

APPROVAL STATEMENT

This report has been reviewed and approved.

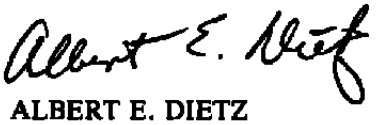

ALBERT E. DIETZ
Directorate of Engineering Development
Deputy for Facilities

Approved for publication:

FOR THE COMMANDER

JERRY C. PULLIAM, Colonel, USAF
Deputy for Facilities

UNCLASSIFIED

SECURITY CLASSIFICATION OF THIS PAGE (When Data Entered)

REPORT DOCUMENTATION PAGE

READ INSTRUCTIONS BEFORE COMPLETING FORM

1. REPORT NUMBER: AEDC-TR-80-58
2. GOVT ACCESSION NO.
3. RECIPIENT'S CATALOG NUMBER

4. TITLE (and Subtitle): MULTIPOLE EXPANSION FOR TRANSIENT ELECTRIC AND MAGNETIC FIELDS IN AN INTERNALLY EXCITED SPHERICAL CAVITY CONTAINING DAMPERS OF FINITE THICKNESS WITH DISTRIBUTED ELECTRICAL PROPERTIES

5. TYPE OF REPORT & PERIOD COVERED: Final Report - Oct. 1, 1979 to Sept. 30, 1980

6. PERFORMING ORG. REPORT NUMBER

7. AUTHOR(s): B. P. Curry, ARO, Inc., a Sverdrup Corporation Company

8. CONTRACT OR GRANT NUMBER(s)

9. PERFORMING ORGANIZATION NAME AND ADDRESS: Arnold Engineering Development Center/DEVM
Air Force Systems Command
Arnold Air Force Station, Tennessee 37389

10. PROGRAM ELEMENT, PROJECT, TASK AREA & WORK UNIT NUMBERS: Program Element 65807F

11. CONTROLLING OFFICE NAME AND ADDRESS: Arnold Engineering Development Center/DOS
Air Force Systems Command
Arnold Air Force Station, Tennessee 37389

12. REPORT DATE: October 1981

13. NUMBER OF PAGES: 54

14. MONITORING AGENCY NAME & ADDRESS (if different from Controlling Office)

15. SECURITY CLASS. (of this report): UNCLASSIFIED

15a. DECLASSIFICATION/DOWNGRADING SCHEDULE: N/A

16. DISTRIBUTION STATEMENT (of this Report)

Approved for public release; distribution unlimited.

17. DISTRIBUTION STATEMENT (of the abstract entered in Block 20, if different from Report)

18. SUPPLEMENTARY NOTES

Available in Defense Technical Information Center (DTIC)

19. KEY WORDS (Continue on reverse side if necessary and identify by block number)

electromagnetic pulse
space chambers
nuclear simulation
multipole expansion
em wave propagation
biconical antennas
nuclear explosion simulation

20. ABSTRACT (Continue on reverse side if necessary and identify by block number)

The multipole expansion coefficients needed to calculate transient electromagnetic fields and cavity frequency response in an internally excited, damped cavity are derived for an arbitrary but centralized distribution of source currents and an arbitrary number of dampers which have finite width. A block matrix procedure is devised to solve the N damper boundary value problems, but specific solutions are presented for the cases of zero, one,

DD FORM 1 JAN 73 1473 EDITION OF 1 NOV 65 IS OBSOLETE

UNCLASSIFIED

SECURITY CLASSIFICATION OF THIS PAGE (When Data Entered)

20. ABSTRACT (Continued)

and two dampers. Also, the TM wave multipole coefficients for an uncapped biconical antenna used as excitation source are obtained in closed form, with use of Schelkunoff's mode solution for the antenna currents. Finally, coupled integrodifferential equations for the current distribution in the end caps and the conical sections of a capped bicone source are presented. This entire theory will be encoded to permit analysis of AEDC experiments.

PREFACE

The work reported herein was conducted by the Arnold Engineering Development Center (AEDC), Air Force Systems Command (AFSC). The results were obtained by ARO, Inc., AEDC Group (a Sverdrup Corporation Company) under ARO Project Number V31K-37. The Air Force project manager was A. E. Dietz. The manuscript was submitted for publication on October 9, 1980.

Mr. B. P. Curry is presently employed by Calspan Field Services, Inc., AEDC Division.

CONTENTS

ILLUSTRATIONS

Figure

Figure | Page

1.0 INTRODUCTION

A recent series of experiments was performed at Arnold Engineering Development Center (AEDC) to investigate the feasibility of improving the quality of System Generated Electromagnetic Pulse (SGEMP) simulation in AEDC space chambers. These experiments, which were carried out in a 12-foot sphere in the von Kármán Gas Dynamics Facility (VKF) at AEDC, have demonstrated that free-space boundary conditions can be simulated in a test chamber by employing suitably designed damping grids to attenuate reflections from the chamber surface. A centrally located, pulsed biconical antenna was used in the experiments as both the source and the detector of transient electromagnetic waves; spherically symmetric dampers were located at various radial positions between the source and the sphere surface, as shown in Fig. 1. The results of these experiments and the damping theory presented in this report will provide a basis for SGEMP facility design.

The purposes of the theoretical treatment developed in this report are to establish a basis for comparing existing experimental data with theoretical predictions, to validate the experiments and theory, and to help determine optimum damping configurations.

Descriptions are presented of the EMP propagation formalism and the methods of solution which will be employed in a computer program to be based on this work. The report does not include a description of the code.

2.0 GENERAL PROPERTIES OF ELECTROMAGNETIC FIELDS

2.1 WAVE PROPAGATION IN A DISSIPATIVE MEDIUM CONTAINING SOURCES

To discuss electromagnetic waves which propagate from a central source region, it is useful to first state Maxwell's equations (in Gaussian units) for fields arising from specified sources embedded in a medium that is isotropic everywhere except at specified interfaces and boundaries (Ref. 1):

$$\nabla \cdot D = 4\pi\rho_c \quad , \quad \overrightarrow{\nabla \times H} = 4\pi \frac{\vec{J}}{c} + \frac{1}{c}\frac{\partial \vec{D}}{\partial t}$$

$$\nabla \cdot B = 0 \quad , \quad \overrightarrow{\nabla \times E} = -\frac{1}{c}\frac{\partial \vec{B}}{\partial t} \tag{1}$$

It is assumed that field quantities and induced quantities are related to each other linearly as

$$\vec{B} = \mu \vec{H} \quad , \quad \vec{D} = \epsilon \vec{E} \quad \text{and} \quad \vec{J} = \sigma \vec{E} + \vec{J}_o \tag{2}$$

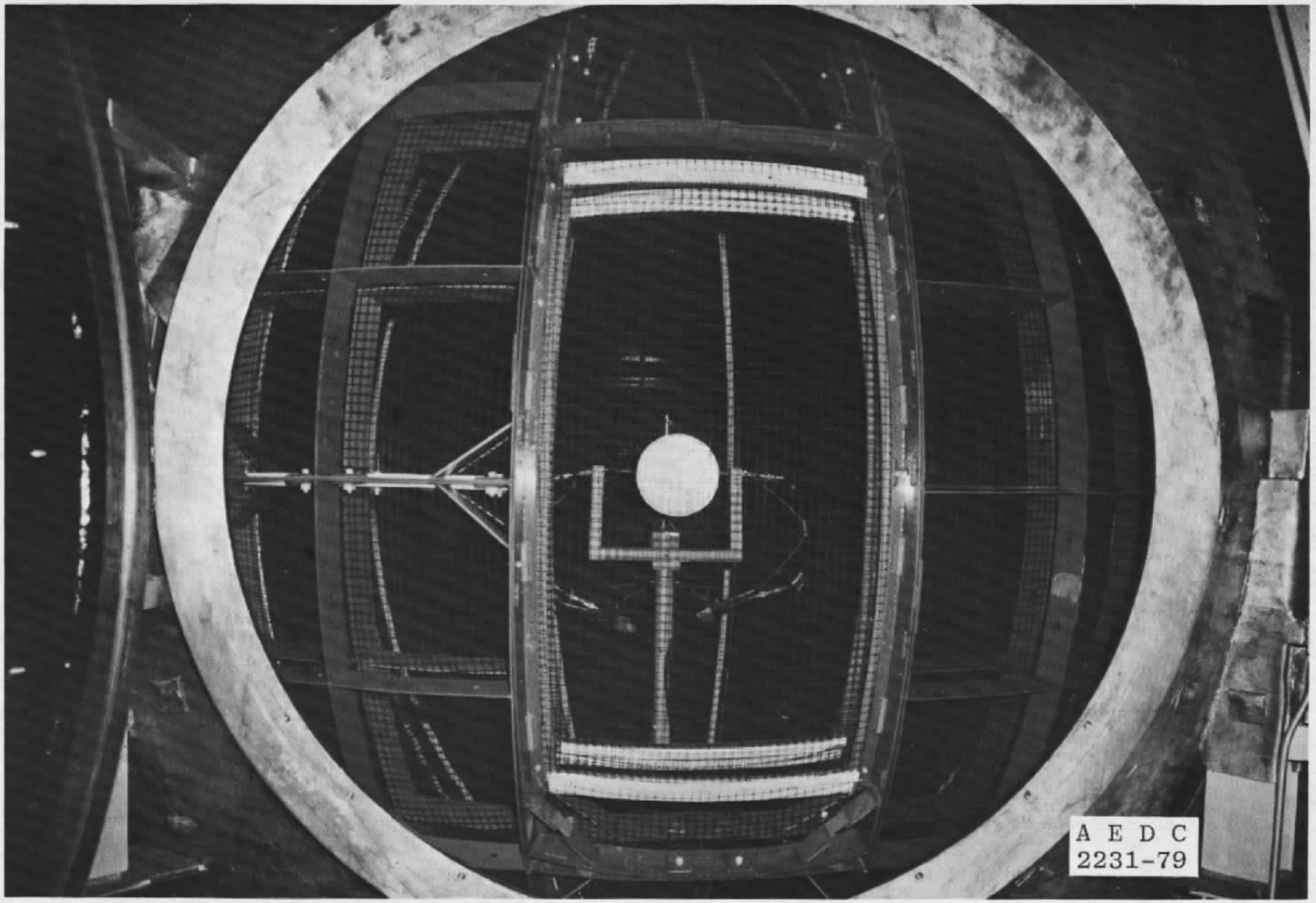

Figure 1. Damping grids installed in VKF 12-ft research sphere.

where μ, ϵ, and σ are, respectively, the magnetic permeability, dielectric permittivity, and electrical conductivity of the medium. It is assumed that the source current density, J_o, and charge density, ϱ_o, exist only within a specified region. In addition, these quantities must satisfy the continuity equation

$$\frac{\partial \rho_e (\vec{r}', t)}{\partial t} + \nabla' \cdot J_o (\vec{r}', t) = 0 \tag{3}$$

where $\vec{r}'$ is a vector from the origin to an infinitestimal element of the source distribution. Using standard vector manipulations (see, for example, Refs. 1 and 2), one can derive the time-dependent electric and magnetic field wave equations from Eqs. (1) and (2).

$$\nabla^2 \vec{E} - \frac{\mu\epsilon}{c^2}\left(\frac{\partial^2 \vec{E}}{\partial t^2} + \frac{4\pi\sigma}{\epsilon}\frac{\partial \vec{E}}{\partial t}\right) = \frac{4\pi\mu}{c^2}\frac{\partial \vec{J}_o}{\partial t} + 4\pi\frac{\overrightarrow{\nabla \rho_e}}{\epsilon}$$

$$\nabla^2 \vec{H} - \frac{\mu\epsilon}{c^2}\left(\frac{\partial^2 \vec{H}}{\partial t^2} + \frac{4\pi\sigma}{\epsilon}\frac{\partial \vec{H}}{\partial t}\right) = -\frac{4\pi}{c}\overrightarrow{\nabla \times J_o} \tag{4}$$

Solution of these equations is greatly facilitated by transformation into the frequency domain, by using the following convention for Fourier transform pairs:

$$\tilde{Q}(\vec{r}, \omega) = \int_{-\infty}^{\infty} Q(\vec{r}, t)\, e^{i\omega t}\, dt$$

$$Q(\vec{r}, t) = \frac{1}{2\pi}\int_{-\infty}^{\infty} \tilde{Q}(\vec{r}, \omega) e^{-i\omega t}\, d\omega \tag{5}$$

In Eq. (5), the functions $\tilde{Q}(\vec{r}, \omega)$ and $Q(\vec{r}, t)$ may be either vectors or scalars, and the use of the tilde over a quantity denotes its evaluation in the frequency domain. The convention used here is that of most modern physics texts. Electrical engineering texts and some optics texts use the convention of replacing "i" with "-i" (sometimes stated as "-j") in Eq. (5) and succeeding equations.

The frequency domain wave equations for the electric and magnetic fields are obtained from Eqs. (3) through (5) and are stated as

$$\nabla^2 \tilde{\vec{E}} + k^2 \tilde{\vec{E}} = -4\pi i\left[\frac{\mu\omega}{c^2}\tilde{\vec{J}}_o + \frac{\vec{\nabla}(\nabla \cdot \tilde{J}_o)}{\omega\epsilon}\right]$$

$$\nabla^2 \tilde{\vec{H}} + k^2 \tilde{\vec{H}} = -\frac{4\pi}{c}\vec{\nabla} \times \tilde{\vec{J}}_o \tag{6}$$

Gradient divergence of the current in the electric field equation results from the occurrence of charge fluctuations in the source region; the gradient divergence causes an essential singularity when Eq. (6) is used to obtain the fields within the source region. We shall see, later, that the singularity can be removed by use of a gauge transformation.

The solutions of Eq. (6) will be stated in terms of Green's functions, which satisfy Helmholtz equations of the form (Ref. 1)

$$\nabla^2 G(\vec{r}, \vec{r}') + k^2 G(\vec{r}, \vec{r}') = -\delta(\vec{r} - \vec{r}') \tag{7}$$

where $\vec{r}$ is a vector from the origin to the field observation point, and $\vec{r}'$ is a vector from the origin to a source point. These Green's functions have the form

$$G(\vec{r}, \vec{r}') = \frac{\exp(ik|r - r'|)}{4\pi|r - r'|} \tag{8}$$

2.2 PROPAGATION CONSTANT, DIELECTRIC CONSTANT, AND WAVE IMPEDANCE

The propagation wave number, k, which appears in Eqs. (6) through (8), is defined by

$$k^2 = \mu\bar{\epsilon}\frac{\omega^2}{c^2} \quad ; \quad \bar{\epsilon} = \epsilon - \frac{4\pi\sigma i}{\omega} \tag{9}$$

where $\bar{\epsilon}$ is the complex dielectric constant characteristic of a dissipative medium. The real and imaginary parts of the propagation constant are stated (Ref. 2) as

$$k_r = \frac{k_o}{\sqrt{2}}\left\{\left[1 + \left(\frac{4\pi\sigma}{\epsilon\omega}\right)^2\right]^{1/2} + 1\right\}^{1/2}$$

$$k_i = \frac{k_o}{\sqrt{2}}\left\{\left[1 - \left(\frac{4\pi\sigma}{\epsilon\omega}\right)^2\right]^{1/2} - 1\right\}^{1/2} \tag{10}$$

In all materials except good conductors, the propagation constant is, approximately, $k = k_o[1 + (2\pi\sigma i)/(\epsilon\omega)]$, where $k_o = \sqrt{\mu\epsilon}\,\omega/c$. By contrast, in good conductors, the propagation constant reduces to $k = (1 + i)/\delta_c$, where δ_c is the skin depth of the conductor, defined as

$$\delta_c = \frac{c}{\sqrt{2\pi\mu\sigma\omega}} \tag{11}$$

It is noteworthy that $\tan^{-1}[(4\pi\sigma)/(\epsilon\omega)]$ is the angle by which displacement current lags behind the true conduction current as a wave propagates through a dissipative medium. A related concept is the impedance presented to the wave by the medium:

$$\tilde{Z} = \frac{4\pi}{c}\sqrt{\frac{\mu}{\epsilon}} = Z_0\left(1 + \frac{4\pi\sigma i}{\epsilon\omega}\right)^{-1/2} \quad . \quad (12)$$

where $Z_0 = (4\pi/c)\sqrt{\mu/\epsilon}$. The impedance of a good conductor is $Z = (1 - i)/(\delta\sigma)$. It is well known that the real part of the impedance is purely resistive, and the sign of the imaginary part (reactance) depends upon whether wave energy is stored capacitively or inductively. The biconical antenna used in the experiments cited earlier is predominantly capacitive, and the dampers are assumed to be purely resistive. The impedance of free space is $Z_{sp} = 4\pi/c = 4.192 \times 10^{-10}$ sec/cm in Gaussian units. [Z_{sp} is equal to 120 π ohms in international units (SI).] In all damping calculations the ratio of the damper impedance to the impedance of the intervening medium occurs; hence, the choice of units is immaterial to the formulation of the multipole expansion boundary value problem.

2.3 ANTENNA IMPEDANCE

The concept of antenna input impedance is considerably different from the wave impedance discussed above. It incorporates the resistive effect related to the loss of energy by radiation. If the antenna were sufficiently long, the effect of the caps could be ignored in computing antenna impedance because the current would be damped (by radiation resistance) enough to suppress reflection of the current pulse from the antenna caps. Since this is not the case at frequencies of interest in the present experiments, the antenna impedance must be computed by dividing the voltage difference between the antenna feed terminals (calculated along an arc of constant radius) by the total current flowing through a circular area whose radius is equal to the antenna terminal radius. Equivalently, one may take twice the voltage difference between the top antenna and the ground plane which bisects the biconical array between the feed terminals (see Fig. 2). The required current can be obtained from the frequency-domain form of Ampere's law.

$$\vec{\nabla} \times \tilde{\vec{H}} = \frac{4\pi}{c}\tilde{\vec{J}} - i\frac{\epsilon\omega}{c}\tilde{\vec{E}} \quad (13)$$

The total current flow is obtained by integrating Eq. (13), using Stokes' theorem

$$I = \int_{\Sigma} \tilde{\vec{J}} \cdot \hat{n}\, d\Sigma = \frac{c}{4\pi}\left[\oint \tilde{\vec{H}} \cdot d\vec{\ell} + i\frac{\epsilon\omega}{c}\int_{\Sigma} \tilde{\vec{E}} \cdot \hat{\gamma}\, d\Sigma\right] \quad (14)$$

where z is along the axis of symmetry and, thus, perpendicular to the ground plane, Σ is the area of a circle whose radius equals the antenna feed radius, and the line integral is evaluated around that circle. Since the current fluxes in the two halves of the antenna are out of phase, the electric field term in Eq. (14) should vanish by symmetry, leaving

$$\tilde{I} = \frac{c}{4\pi} \oint \tilde{\vec{H}} \cdot d\vec{\ell} = \lim_{r \to \delta} \frac{c}{2} r \sin \theta_c \tilde{H}_\phi (r, \theta, \phi = 0) \tag{15}$$

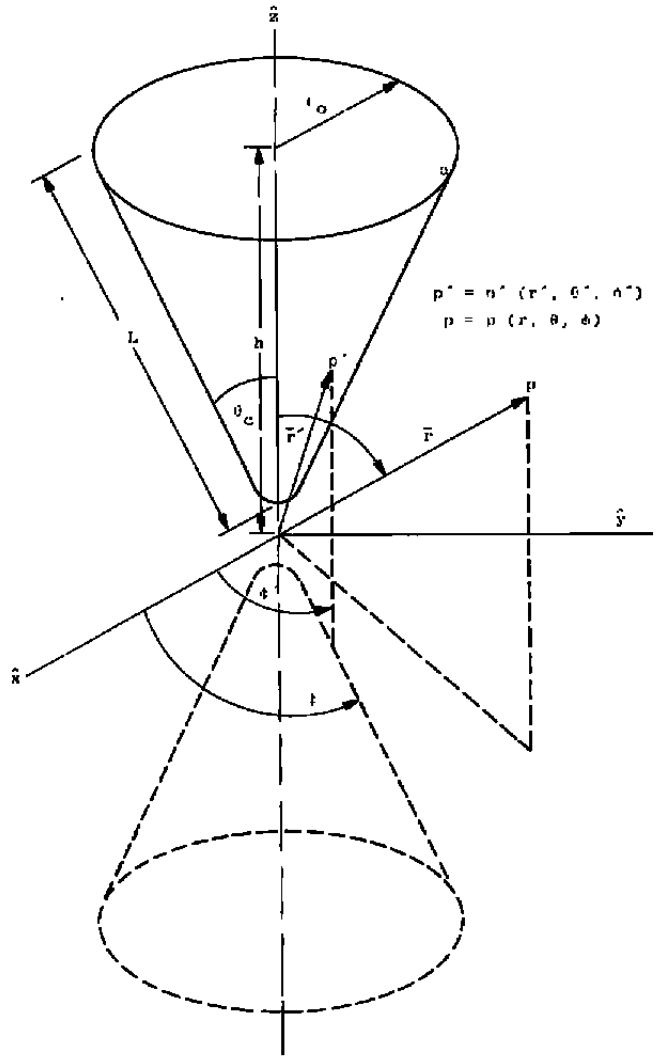

Figure 2. Coordinate system for the electrical description of a biconical antenna.

where $\delta \sin \theta_c$ is the feed radius of the antenna, and θ_c is the antenna half-cone angle. The voltage difference between the two halves is just

$$\tilde{V} = 2 \int_{\theta = \theta_c}^{\pi/2} \tilde{E} \cdot d\vec{\ell} = 2 \left[r \int_{\theta_c}^{\pi/2} \tilde{E}_\theta (r, \theta, \phi = 0)\, d\theta \right]_{r \to \delta} \tag{16}$$

Thus, the antenna impedance is

$$\tilde{Z}_A = \tilde{V}/\tilde{I} = \frac{4}{c} \frac{\int_{\theta_c}^{\pi/2} \tilde{E}_\theta (\delta, \theta, \phi = 0)\, d\theta}{\sin \theta_c \, \tilde{H}_\phi (\delta, \theta_c, \phi = 0)} \tag{17}$$

In these equations, the fields are evaluated at $\phi = 0$ (for convenience) since there is axisymmetry. Through the multipole expansion which will be developed later, Eq. (17) contains both the effect of the source characteristics and the damping and reflecting properties of the cavity. In fact, the antenna impedance for free-space boundary conditions can be obtained simply by setting the multipole coeffieients that represent standing waves in the region between the source and the first damper equal to zero for Eq. (17).

2.4 FREQUENCY RESPONSE OF THE ANTENNA-CAVITY SYSTEM

After the fields have been obtained and Eq. (17) has been evaluated, the frequency response of the entire system (antenna plus chamber with damping grids) is obtained (assuming that there are no losses in the transmission line and that it is perfectly matched to the antenna) from transmission line theory (Ref. 3).

$$\frac{\tilde{I}_{out}(\omega)}{\tilde{I}_{in}(\omega)} = \frac{Z_A(\omega) - Z_c}{Z_A(\omega) + Z_c} \tag{18}$$

where $Z_c = (Zsp/\pi)$ ℓn cot $(\theta_c/2)$ is the (purely resistive) characteristic impedance of the antenna. The procedure for comparing theory and experiments is, thus, the following:

1. Obtain the Fourier transform of the input current pulse (prior to the arrival of the first reflection from the cavity).
2. Calculate the electric and magnetic fields from the multipole expansion which will be derived later. (This step is optional and may be omitted if only the sensed pulse waveform is desired.)
3. Calculate the system frequency response from Eqs. (17) and (18).

4. Calculate the inverse Fourier transform I_{out} (t) of the current measured at the antenna terminals. This result can then be compared with the experimental pulse waveform. In performing Step (4), one must account for contributions to I_{out} (t) from the negative frequency domain of I_{out} (ω) as well as from the domain of positive frequencies.

3.0 SOLUTION OF THE ELECTROMAGNETIC FIELD WAVE EQUATIONS BY USE OF HERTZ-DEBYE POTENTIALS

The use of Hertz-Debye potentials yields an automatic separation of the solutions of Eq. (6) into TM and TE waves. Another advantage of using these potentials is their value as an intermediary in the determination of all electric and magnetic field components from the radial inhomogeneous solutions of Eq. (6). Formal mathematical properties of these potentials are discussed extensively in Ref. 4. These potentials are introduced here in a fashion analogous to that of Ref. 2 (pp. 28 — 30); however, the treatment presented here is generalized to include dissipative effects.

3.1 SOLUTION OF THE HOMOGENEOUS WAVE EQUATIONS

The Hertz vectors $\vec{P}_E$ ($\vec{r}$, t) and $\vec{P}_M$ ($\vec{r}$, t) are introduced as particular solutions to the source free form of Eq. (1):

$$\vec{H}_1 = \frac{c}{\epsilon} \vec{\nabla} \times \frac{\partial \vec{P}_E}{\partial t}$$

$$\vec{E}_2 = -\frac{\mu}{c} \vec{\nabla} \times \frac{\partial \vec{P}_M}{\partial t} \tag{19}$$

Additional particular solutions of Eq. (1) are obtained by substituting Eq. (19) into Eq. (1), yielding, for the electric field:

$$\left(\frac{\partial}{\partial t} + \frac{4\pi\sigma}{\epsilon}\right)\vec{E}_1 = \vec{\nabla} \times \left(\vec{\nabla} \times \frac{\partial \vec{P}_E}{\partial t}\right) \tag{20}$$

and

$$\overrightarrow{\nabla \times E_1} = -\frac{\mu\epsilon}{c^2} \nabla \times \frac{\partial^2 \vec{P}_E}{\partial t^2}$$

The analogous equations for $\vec{H}_2$ are

$$\frac{\partial \vec{H}_2}{\partial t} = \vec{\nabla} \times \left(\vec{\nabla} \times \frac{\partial \vec{P}_M}{\partial t} \right) \tag{21}$$

and

$$\overrightarrow{\nabla \times H_2} = - \frac{\mu\epsilon}{c^2} \left(\frac{\partial}{\partial t} + \frac{4\pi\sigma}{\epsilon} \right) \vec{\nabla} \times \frac{\partial \vec{P}_m}{\partial t}$$

Wave equations analogous to Eq. (4) are obtained by use of the following procedure:

1. The terms $-\vec{\nabla}(\nabla \cdot \partial P_E/\partial_t)$ and $-\vec{\nabla}(\nabla \cdot \partial P_M/\partial t)$ are added to the first E_1 equation and the first H_2 equation, respectively. Since the curl of the gradient vanishes, this addition does not alter the results of the next operation and is, in fact, equivalent to a gauge transformation.

2. The second operation consists of taking the curl of the first $\vec{E}_1$ equation and the first $\vec{H}_2$ equation, as well as the time derivative of the second $\vec{H}_2$ equation. $\vec{E}_1$, $\vec{E}_2$, $\vec{H}_1$, and $\vec{H}_2$ are eliminated from the resulting four equations, to obtain the homogeneous wave equations for the Hertz vectors $\vec{P}_E$ and $\vec{P}_M$ in the time domain

$$\vec{\nabla} \times \left[\frac{\mu\epsilon}{c^2} \left(\frac{\partial}{\partial t} + \frac{4\pi\sigma}{\epsilon} \right) \frac{\partial \vec{P}_E}{\partial t} - \nabla^2 \vec{P}_E \right] = 0$$

$$\vec{\nabla} \times \left[\frac{\mu\epsilon}{c^2} \left(\frac{\partial}{\partial t} - \frac{4\pi\sigma}{\epsilon} \right) \frac{\partial \vec{P}_M}{\partial t} - \nabla^2 \vec{P}_M \right] = 0 \tag{22}$$

The electric and magnetic fields are constructed from $\vec{E} = \vec{E}_1 + \vec{E}_2$ and $\vec{H} = \vec{H}_1 + \vec{H}_2$, where $\vec{E}_1$ is obtained by inverting the first part of Eq. (20) and $\vec{E}_2$ is given by the second part of Eq. (19). Similarly, $\vec{H}_1$ is given by the first part of Eq. (19), and $\vec{H}_2$ is obtained by inverting the first part of Eq. (21). This process is greatly facilitated by Fourier transformation. The electric and magnetic fields in the frequency domain are, thus, derived from the corresponding Hertz vectors as stated below:

$$\tilde{\vec{E}} = \frac{\vec{\nabla} \times \left(\vec{\nabla} \times \tilde{\vec{P}}_E \right)}{1 - \frac{4\pi\sigma_1}{\epsilon\omega}} + i \frac{\mu\omega}{c} \vec{\nabla} \times \tilde{\vec{P}}_M$$

and

$$\vec{H} = \vec{\nabla} \times \left(\vec{\nabla} \times \tilde{\vec{P}}_M \right) - i \frac{\epsilon\omega}{c} \vec{\nabla} \times \tilde{\vec{P}}_E \tag{23}$$

The utility of the Hertz-Debye formalism is made immediately apparent upon examination of these equations. If the vectors $\vec{P}_E$ and $\vec{P}_M$ are assumed to be radial in form, then the curl of each vector can have no radial component. Hence, the electric field derived from $\vec{P}_M$ and the magnetic field derived from $\vec{P}_E$ are entirely transverse. Because of the terms involving the curl of the Hertz vectors, the electric field derived from $\vec{P}_E$ and the magnetic field derived from $\vec{P}_M$ have nonvanishing radial components. For this reason, the fields derived from the electric Hertz-Debye potentials are called transverse magnetic (TM) waves. Similarly, the magnetic Hertz-Debye potential is the source of transverse electric (TE) waves. These potentials are defined by

$$\vec{P}_E(\vec{r}, t) = \vec{r}\,\pi_E(\vec{r}, t)$$

and

$$\vec{P}_M(\vec{r}, t) = \vec{r}\,\pi_M(\vec{r}, t) \tag{24}$$

It should be noted that the separation of fields into TM and TE waves by use of these potentials is independent of the choice of coordinate system.

The wave equation satisfied by the Hertz-Debye potentials is derived by use of the following vector identities:

$$\overrightarrow{\nabla \times r} = 0, \quad \nabla^2(\vec{r}\,s) = 2\vec{\nabla}s$$

and

$$\vec{\nabla} \times (\vec{r}\,s) = \vec{\nabla}s \times \vec{r}$$

where s is any scalar. Equation (22) can now be reduced to the form

$$\vec{\nabla} S \times \vec{r} = 0$$

where

$$S = \frac{\mu\epsilon}{c^2}\left(\frac{\partial}{\partial t} + \frac{4\pi\sigma}{\epsilon}\right)\frac{\partial \pi_{E,M}}{\partial t} - \nabla^2 \pi_{E,M}$$

An equation of this type is satisfied either by S = 0 or S as a function only of r. The second choice is trivial; the first yields the scalar wave equations for the Hertz-Debye potentials in the time domain

$$\frac{\mu\epsilon}{c^2}\left(\frac{\partial}{\partial t} + \frac{4\pi\sigma}{\epsilon}\right)\frac{\partial \pi_{E,M}}{\partial t} - \nabla^2 \pi_{E,M} = 0 \tag{25}$$

for either the electric or magnetic Hertz-Debye potential. Fourier transformation yields the corresponding scalar Helmholtz equations in the frequency domain:

$$\nabla^2 \tilde{\pi}_{E,M} + k^2 \tilde{\pi}_{E,M} = 0 \tag{26}$$

3.1.1 Spherical Coordinate Representation of the Electric and Magnetic Fields Derived from the Hertz-Debye Potentials

The spherical coordinate decomposition of Eq. (23) is essential for two reasons: (1) to permit the definition of the boundary value problem posed by the dampers in the spherical cavity and (2) to facilitate solution of the inhomogeneous field equations, Eq. (6). The latter is accomplished by a treatment similar to that of Ref. 4, using the properties of the angular momentum operator L^2, which is the angular portion of the Laplacian operator ∇^2 (detailed in Section 3.2). To facilitate the decomposition of Eq. (23), it is convenient to use the following vector identities:

$$\vec{\nabla} \times \left(\vec{\nabla} s \times \vec{r} \right) = 2 \vec{\nabla} s + r \cdot \nabla \left(\vec{\nabla} s \right) - \vec{r} \ \nabla^2 s$$

and

$$\nabla^2 s = \frac{1}{r} \frac{\partial^2 (rs)}{\partial r^2} \frac{L^2}{r^2} s$$

where the scalar, s, is taken to be either $\tilde{\pi}_E$ or $\tilde{\pi}_M$.

The electric and magnetic fields derived from the Hertz-Debye potentials can now be stated, quite simply, as

$$\tilde{\vec{E}} = \hat{r} \frac{L^2}{r} \frac{\tilde{\pi}_E}{\left(1 + \frac{4\pi\sigma i}{\epsilon\omega}\right)} + \frac{\theta}{r} \left[\frac{i\mu\omega}{c \sin\theta} \frac{\partial r \tilde{\pi}_M}{\partial \phi} + \left(1 + \frac{4\pi\sigma i}{\epsilon\omega}\right)^{-1} \frac{\partial^2 r \tilde{\pi}_E}{\partial r \, \partial \theta} \right]$$

$$- \frac{\hat{\phi}}{r} \left[\frac{i\mu\omega}{c} \frac{\partial r \tilde{\pi}_M}{\partial \theta} - \frac{\left(1 + \frac{4\pi\sigma i}{\epsilon\omega}\right)^{-1}}{\sin\theta} \frac{\partial^2 r \tilde{\pi}_E}{\partial r \, \partial \phi} \right] \tag{27}$$

and

$$\tilde{\vec{H}} = \hat{r} \frac{L^2 \pi_M}{r} - \frac{\hat{\theta}}{r} \left[\frac{i\epsilon\omega}{c} \frac{\partial r \tilde{\pi}_E}{\partial \phi} - \frac{\partial^2 r \tilde{\pi}_M}{\partial r \, \partial \theta} \right]$$

$$+ \frac{\hat{\phi}}{r} \left[\frac{i\epsilon\omega}{c} \frac{\partial r \tilde{\pi}_E}{\partial \theta} + \frac{1}{\sin\theta} \frac{\partial r \tilde{\pi}_M}{\partial r \, \partial \phi} \right] \tag{28}$$

Analogous equations could be stated for other choices of geometry by expanding Eq. (22) in the appropriate coordinate system.

3.1.2 Boundary Conditions on the Hertz-Debye Potentials

The boundary conditions which are imposed at each interface shown in Fig. 3 are continuity of tangential electric and magnetic field components, $\vec{r} \times \tilde{\vec{E}}$ and $\vec{r} \times \tilde{\vec{H}}$. Let us denote by r_j^- the approach to the "j*th*" interface from outside that interface — i.e., $r_j^+ = r_j + \zeta$, where ζ is a positive infinitesimal. Similarly, let $r_j^- = r_j - \zeta$ denote the approach to the interface from inside it. Referring to Eqs. (27) and (28), we find that the following four matching conditions must be satisfied at each interface:

$$\left[\mu \tilde{\pi}_M\right]_{r \to r_j^-} = \left[\mu \tilde{\pi}_M\right]_{r \to r_j^+}$$

$$\left[\epsilon \tilde{\pi}_E\right]_{r \to r_j^-} = \left[\epsilon \tilde{\pi}_E\right]_{r \to r_j^+}$$

$$\left[\frac{\partial r \tilde{\pi}_M}{\partial r}\right]_{r \to r_j^-} = \left[\frac{\partial r \tilde{\pi}_M}{\partial r}\right]_{r \to r_j^+}$$

$$\left[\frac{\partial}{\partial r}\left(r \tilde{\pi}_E\right) \Big/ \left(1 + \frac{4\pi\sigma i}{\epsilon\omega}\right)\right]_{r \to r_j^-} = \left[\frac{\partial}{\partial r}\left(r \tilde{\pi}_E\right) \Big/ \left(1 - \frac{4\pi\sigma i}{\epsilon\omega}\right)\right]_{r \to r_j^+} \tag{29}$$

In a later section, the multipole expansion of the Hertz-Debye potentials will be presented, and a matrix procedure based on Eq. (29) will be used to relate the multipole coefficients in all the regions shown in Fig. 3.

3.2 SOLUTION OF THE INHOMOGENEOUS WAVE EQUATIONS BY USE OF THE HERTZ-DEBYE POTENTIALS AND SOURCE GREEN'S FUNCTIONS

With reference to the vector identity

$$\nabla^2 (V \cdot r) = \vec{r} \cdot \nabla^2 \vec{V} + 2 \nabla \cdot V$$

(where $\vec{V}$ is either $\tilde{\vec{E}}$ or $\tilde{\vec{H}}$), we can show that the radial components of Eq. (6) must satisfy

$$\nabla^2 (\tilde{E} \cdot r) + k^2 (\tilde{E} \cdot r) = -i \frac{Z_o}{k_o} \left[k_o^2 \tilde{J}_o \cdot r + \left(2 + \tilde{r} \frac{\partial}{\partial r} \right) \nabla \cdot \tilde{J}_o \right] \tag{30}$$

where $Z_o = (4\pi/c)/(\sqrt{\mu/E})$ is the (real) impedance of the medium (which will usually be free space) outside the source, and

$$\nabla^2 (\tilde{H} \cdot r) + k^2 (\tilde{H} \cdot r) = -\frac{Z_{sp}}{\sin \theta} \left[\frac{\partial (\sin \theta \, \tilde{J}_o \cdot \hat{\phi})}{\partial \theta} - \frac{\partial \tilde{J}_o \cdot \hat{\theta}}{\partial \phi} \right] \tag{31}$$

where $Z_{sp} = 4\pi/c$ is the impedance of free space. In what follows it is useful to write the Laplacian operator as $\nabla^2 s = [(L^2 s)/r^2] + 1/r(\partial^2 rs)/(\partial r^2)$ where $\vec{L} = -i \vec{r} \times \vec{\nabla}$ is the angular momentum operator. This operator is extensively used in both classical and quantum mechanical studies, and its properties (in the context of radiation fields) are discussed in detail in Refs. 1 and 4. The eigenfunctions of L^2 are $\ell(\ell+1)$. The solutions of Eq. (26) are constructed for a spherical geometry from

$$k r \tilde{\pi}_{E, M} = \sum_{\ell, m} C_\ell^m Y_\ell^m (\theta, \phi) \left[\zeta_\ell^1 (k r), \zeta_\ell^2 (k r), \psi_\ell (k r) \right] \tag{32}$$

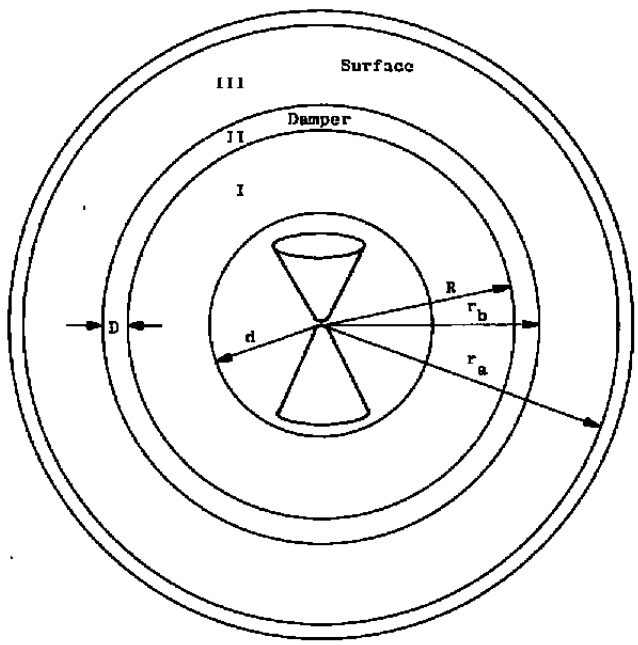

Figure 3. Geometry for electromagnetic wave propagation in an internally excited hollow sphere containing a single damping region.

where $\{C_\ell^m\}$ denotes a set of multipole expansion coefficients which will later be determined for each region of the cavity shown in Fig. 1. The functions $\zeta_\ell^1(kr)$, $\zeta_\ell^2(kr)$, and $\psi_\ell(kr)$ are, respectively, Ricatti-Hänkel functions of the first and second kind and Ricatti-Bessel functions. $\zeta_\ell^1(kr)$ and $\zeta_\ell^2(kr)$ represent, respectively, outwardly and inwardly propagating spherical waves and $\psi_\ell(kr)$ represents standing waves (in undamped regions of the cavity). The asymptotic limits of the Ricatti-Hänkel and Ricatti-Bessel functions are, respectively,

$$\underset{r \to \infty}{\lim} \zeta_\ell^{1,2}(kr) = \exp\left\{\pm i\left[kr - \frac{\pi}{2}(\ell+1)\right]\right\} \quad \text{and} \quad \underset{r \to \infty}{\lim} \psi_\ell(kr) = \sin\left(kr - \frac{\pi}{2}\ell\right)$$

Only the functions $\psi_\ell(kr)$ are regular at the origin; hence, only these functions can be used within the source region. Properties of these functions are discussed in Ref. 5.

The solutions of Eqs. (30) and (31) are obtained by use of the Green's function, which satisfies Eq. (7). These solutions are then related to the corresponding Hertz-Debye potentials through the radial components of Eqs. (27) and (28). The results are

$$L^2(\tilde{\pi}_E)\Big/\left(1 + \frac{4\pi\sigma i}{\epsilon\omega}\right) = \tilde{E}\cdot r = i\tilde{Z}k \int_{V'} \left[\tilde{J}_o \cdot r' + \left(2 + r'\frac{\partial}{\partial r'}\right)\frac{\nabla'\cdot\tilde{J}_o}{k_o^2}\right] G(\vec{r}, \vec{r}')\, d^3\vec{r}' \tag{33}$$

where $\tilde{Z}$ is the wave impedance defined in Eq. (12), and

$$L^2(\tilde{\pi}_M) = \tilde{H}\cdot r = Z_{sp}\int_{V'}\left[\frac{\partial}{\partial\theta'}(\sin\theta' \tilde{J}_o\cdot\hat{\phi}') - \frac{\partial(J_o\cdot\hat{\theta}')}{\partial\phi'}\right]\frac{G(\vec{r}, \vec{r}')}{\sin\theta'}\, d^3\vec{r}' \tag{34}$$

where V′ is the smallest volume completely enclosing the source distribution and is not necessarily spherical, and the Green's function is defined in Eq. (8).

The potentials in Eqs. (33) and (34) have the form

$$kr\,\pi_{E,M} = \sum_{\ell,m}\left(a_\ell^m, b_\ell^m\right) Y_\ell^m(\theta, \phi)\, \zeta_\ell^1(kr) \tag{35}$$

where $\{a_\ell^m\}$ and $\{b_\ell^m\}$ denote the sets of source multipole coefficients for TM waves and TE waves, respectively.

The Green's functions in Eqs. (33) and (34) are expanded (Ref. 1)* in terms of the Ricatti-Bessel functions and spherical harmonics as

$$G(\vec{r}, \vec{r}\,') = \frac{\vec{r}}{kr'r} \sum_{\ell, m} \psi_\ell(kr') \zeta_\ell^1(kr) Y_\ell^{m'}(\theta', \phi') Y_\ell^m(\theta, \phi) \tag{36}$$

With use of this expansion and the orthogonality properties of the spherical harmonics, the source multipole coefficients may be obtained for TM and TE waves by premultiplying Eqs. (33) and (34) by $Y_\ell^{m*}(\theta,\phi)$ and integrating over a normalizing sphere.

The result for the TM wave source multipole expansion coefficients is

$$a_\ell^m = -\frac{\tilde{Z}}{\ell(\ell+1)} \frac{k^3}{k_o^2} \iiint_{V'} \left[\tilde{J}_o \cdot r' + \left(2 + r' \frac{\partial}{\partial r'}\right) \frac{\nabla' \cdot \tilde{J}_o}{k_o^2} \right] \frac{\psi_\ell(kr')}{r'} Y_\ell^{m*}(\theta', \phi')\, d^3\vec{r}\,' \tag{37}$$

where* denotes complex conjugate. Similarly, the TE wave source multipole coefficients are

$$b_\ell^m = \frac{i Z_{s_p}}{\ell(\ell+1)} \iiint_{V'} \left[\frac{\partial}{\partial \theta'} (\sin\theta' \tilde{J}_o \cdot \hat{\phi}') - \frac{\partial}{\partial \phi'} (\tilde{J}_o \cdot \hat{\theta}') \right] \frac{\psi_\ell(kr')}{r' \sin\theta} Y_\ell^{m*}(\theta' \phi')\, d^3\vec{r}\,' \tag{38}$$

Equations (37) and (38) are valid for a general source distribution. For an axisymmetric source, however, TE waves vanish and the TM wave coefficients reduce, outside a spherical region completely enclosing the sources, to

$$a_\ell^m \to a_\ell = -\frac{\sqrt{\pi(2\ell+1)}}{\ell(\ell+1)} \tilde{Z} \frac{k^3}{k_o^2} \iint \left[r'^2 \tilde{J}_o \cdot \hat{r}'\, \psi_\ell(kr') - \frac{k}{k_o^2} \psi_\ell'(kr') \frac{\partial}{\partial r'} \left(r'^2 \nabla' \cdot \tilde{J}_o \right) \right]$$

$$P_\ell(\cos\theta') \sin\theta' d\theta' dr' \tag{39}$$

*The Green's function expansion stated in Ref. 1 involves the spherical Bessel functions $J_\ell(kr)$ and spherical Hankel functions $h_\ell^2(kr)$. The Ricatti functions are simply the products of these functions with their arguments.

Obviously, one must know the source current distribution to use these equations. Equations (37) and (38) are presented because of the necessity to consider arbitrary source currents when satellite components are irradiated in a test chamber. In the next section, Eq. (39) will be evaluated for an uncapped biconical antenna. In addition, rigorous coupled integro-differential equations will be derived in order to calculate the current distribution characteristic of a capped biconical antenna. In succeeding sections, the cavity boundary value problem will be solved and the resulting regional multipole coefficients will be related to the source multipole coefficients stated in Eqs. (37) and (38).

3.2.1 Source Multipole Expansion for an Uncapped Biconical Antenna Radiating into an Unbounded Medium

Although its use in analyzing the existing test chamber results requires that Eq. (36) should incorporate the current distribution calculated (with the equations presented in the next section) for a capped bicone, some of the properties of the source multipole coefficients can be demonstrated by evaluating Eq. (39) for a specific current distribution: Schelkunoff's mode solution (Ref. 6) for an uncapped bicone. For this case, Eq. (39) can be evaluated in closed form. Referring to Fig. 2, we consider a system of two cones generated by revolution of the line segment d-δ about the positive and negative z-axes. We shall require that the radial gap, 2δ, between the cones be small.

The form assumed for the current distribution is purely radial:

$$\tilde{\vec{J}}_o(\vec{r}\,') = \frac{\hat{r}'}{2\pi r'^2} \sum_{i=1}^{3} \tilde{I}_o^{(i')}(\omega, r') \left[\delta(\cos\theta - \cos\theta_c) - \delta(\cos\theta + \cos\theta_c)\right] \qquad (40)$$

This form is a generalization of the current distribution stated in Ref. 1 for a thin, linear antenna. The primary current mode is sinusoidal:

$$\tilde{I}_o^{(1)}(\omega, r') = \tilde{I}_o(\omega) \sin\left[k_o(d - r')\right]$$

The reflected mode is

$$\tilde{I}_o^{(2)}(\omega, r') = -i\,\tilde{I}_o(\omega)\,\frac{Z_A}{Z_c}\cos\left[k_o(d - r')\right]$$

and its contribution to Eq. (39) vanishes. The higher-order modes, which arise from the reaction of the radiated fields on the antenna, are stated (from Ref. 6) as*

$$\tilde{I}_o^{(3)}(\omega, r') = \frac{i\tilde{I}_o(\omega)}{2\pi} \frac{Z_{s_p}}{Z_c} \sum_{\ell=0}^{\infty} \frac{4\ell+3}{(\ell+1)(2\ell+1)} \zeta_{2\ell+1}^{1}(kd)\, \psi_{2\ell+1}(k_o r') \quad (41)$$

The reader should note that $\tilde{I}_o(\omega)$ is *not* the current measured at the input terminals. It is a complex quantity which is related to the input current and voltage by the following pair of equations:

$$\tilde{I}(\omega, \delta) = \tilde{I}_o(\omega)\left[\sin(kd) - i\frac{Z_A}{Z_c}\cos(kd)\right]$$

and

$$\tilde{V}(\omega, \delta) = \tilde{I}_o(\omega)\left[Z_A \sin(kd) - i Z_c \cos(kd)\right] \quad (42)$$

The antenna impedance in these equations is also obtained from Schelkunoff's mode solution:

$$Z_A = i Z_c \left[\tilde{I}_o^{(3)}(\omega, r')/\tilde{I}_o(\omega)\right]_{r' \to d} \quad (43)$$

The form of the current distribution in Eq. (40) can be exploited to cast Eq.(39) into the following useful equation, in the fashion of Ref. 1.

$$a_\ell = \sqrt{\frac{2\ell+1}{\pi}}\left[\frac{1-(-1)^\ell}{2}\right]\frac{P_\ell(\cos\theta_c)}{\ell(\ell+1)}\tilde{Z}\frac{k^3}{k_o^2}$$

$$\times \int_\delta^d \left\{\left[I_o(\omega, r') + \frac{1}{k_o^2}\frac{d^2\tilde{I}_o(\omega, r')}{dr'^2}\right]\psi_\ell(kr') - \frac{1}{k_o^2}\frac{d}{dr'}\left[\frac{d\tilde{I}_o(\omega, r')}{dr'}\psi_\ell(kr')\right]\right\} dr' \quad (44)$$

*Because of the choice of outgoing boundary conditions in Ref. 6, $\zeta_{2\ell+1}^2(kd)$ appears in the complementary current modes, and there is no distinction between k and k_o.

where

$$\tilde{I}_o(\omega, r') = \sum_{i=1}^{3} \tilde{I}_o^{(i)}(\omega, r')$$

Note that only odd ℓ multipoles occur because of the symmetry of the bicone. Insertion of the three current modes stated in Eq. (39) into Eq. (46) yields (as $k\delta \to 0$)

$$a_\ell = \sum_\ell \sqrt{\frac{2\ell+1}{\pi}} \left[\frac{1-(-1)^\ell}{2}\right] \frac{P_\ell(\cos\theta_c)}{\ell(\ell-1)} Z_o \frac{k^2}{k_o^2} \tilde{I}_o(\omega) \psi_\ell(kd)$$

$$\cdot \left[1 - i \frac{Z_{s_p}}{Z_c} \sum_{n=o}^{\infty} \frac{4n+3}{(n+1)(2n+1)} \frac{\zeta^1_{2n+1}(kd)}{\psi_\ell(kd)} J_{n,\ell}\right] \tag{45}$$

where

$$J_{n,\ell} \equiv k_o \int_\delta^d \left[\psi_{2n+1}(k_o r') \psi_\ell(k r') - \frac{k}{k_o} \psi'_{2n+1}(k_o r') \psi'_\ell(k r')\right] dr'$$

The remaining integral can be evaluated by using the properties of the Ricatti-Bessel functions and Bessel function integrals and recursion relations stated in Ref. 5. After much tedious mathematical manipulation, we find

$$J_{n,\ell} = \frac{2(n+1)}{2n+\ell-2} \left\{ \frac{2n+1}{2n+1-\ell} \left(\frac{k^2}{k_o^2} - 1\right) k_o \int_o^d \psi_\ell(k r') \psi_{2n+1}(k_o r') dr' \right.$$

$$- (\ell-1) \psi_\ell(kd) \frac{\psi_{2n+1}(k_o d)}{k_o d}$$

$$\left. + \frac{1}{2n+1-\ell} \left[\frac{\ell(\ell+1)}{2(n-1)} \psi_\ell(kd) \psi_{2n+2}(k_o d) - (2n+1) \frac{k}{k_o} \psi_{\ell+1}(kd) \psi_{2n+1}(k_o d)\right]\right\} \tag{46}$$

Assuming that $|(k^2/k_o^2) - 1| << 1$, we obtain the final form for the source multipole coefficients of an uncapped biconical antenna:

$$a_\ell = \sqrt{\frac{2\ell+1}{\pi}} \left[\frac{1-(-1)^\ell}{2}\right] \frac{P_\ell(\cos\theta_c)}{\ell(\ell+1)} Z_o \frac{k^2}{k_o^2} \tilde{I}_o(\omega) \psi_\ell(kd) \left[1 + i \underset{\sim}{X}_\ell(k, k_o, d)\right] \tag{47}$$

where $\chi_\ell(k, k_o, d)$ is denoted the "complementary antenna function" and is defined, in accordance with Eq. (46), as

$$X_\ell(k, k_o, d) = \frac{Z_{s_p}}{\pi Z_c} \sum_{n=0}^{\infty} \frac{4n-3}{2(n+1)+\ell} \zeta_\ell^1(kd) \left\{ (\ell+1) \frac{\psi_{2n-1}(k_o d)}{(k_o d)} \right.$$

$$\left. - \frac{1}{2n+1-\ell} \left[\frac{\ell(\ell-1)}{2(n+1)} \psi_{2n+2}(k_o d) - (2n+1) \frac{k}{k_o} \frac{\psi_{\ell-1}(kd)}{\psi_\ell(kd)} \psi_{2n-1}(k_o d) \right] \right\} \tag{48}$$

It is interesting to note from Eq. (47) that the contribution of the complementary current modes to the source multipoles is out of phase with the contribution of the primary mode. Since these equations are closed-form expressions, their evaluation permits a check on the source coefficients obtained from the numerical solutions of the more general capped bicone integrodifferential equations derived in the next section.

3.2.2 Derivation of the Coupled Integrodifferential Equations for the Current Distribution on a Capped Biconical Antenna Radiating into an Unbounded Medium

The presence of caps on the bicone complicates the treatment of the last section. In this section, the equations describing the radial current distribution in the conical sections of the antenna and the expanding and contracting current circles in the end caps are derived by treating the antenna as a boundary value problem and using a gauge transformation to treat the singularities which occur in Eq. (39) when the observation and source points coincide ($\vec{r} \rightarrow \vec{r}'$). Using this transformation introduces the effect of an accumulation of fluctuating charge near the antenna tips. Conservation of current (Kirchoff's law) at the cone-cap juncture prevents charge accumulation at the caps.

The boundary value problem is posed by requiring the tangential electric fields on the antenna surfaces to vanish, assuming that the surfaces are perfect conductors. Referring to Fig. 2, we can see that the vanishing of the electric field on the conical parts of the antenna is expressed by

$$\hat{\theta} \times \vec{E} = \hat{r} E_\phi - \hat{\phi} E_r = -\hat{\phi} E_r = 0 \quad \text{at } \theta = \theta_c \text{ and } \pi - \theta_c, \text{ and for } \delta \leq r \leq d,$$

at $\theta = \theta_c$ and $\pi - \theta_c$, and for $\delta \leq r \leq d$, where $2\delta \cos \theta_c$ is the axial separation distance between the cones. The azimuthal field, E_ϕ, vanishes by symmetry. The radial field, E_r, contains contributions from both the cones and the end caps.

Similarly, the tangential field on the end caps is given by

$$\hat{z} \times \vec{E} = \hat{\phi} E_\rho - \hat{\rho} E_\phi = \hat{\phi} E_\rho$$

where ϱ, θ, and ϕ are cylindrical coordinates describing the antenna, and the tangential field is evaluated at $z = \pm h$ for $0 \leq \varrho \leq \varrho_0$. This field also contains contributions from sources on both the cones and end caps.

The solution of the first part of Eq. (6) is obtained by using properly selected singular Green's functions. Caution is required, however, because of the gradient of the divergence of the current density in the first part of Eq. (6). If this term appears inside the source integral, as in Eq. (39), there results a non-integrable singularity (Ref. 7) when observation and source points coincide; consequently, the treatment of Section 3.2.0 cannot be used to describe the fields on the antenna surface.* We shall instead transform the field in such a way that the divergence of the current density appears inside the integral and the gradient appears outside (as in Ref. 7). Such a transformation is equivalent to the specification of the gauge condition for the conventional vector and scalar potentials.

Let the transformation be

$$\tilde{\vec{E}} = \vec{U} + \vec{\nabla} \psi \tag{49}$$

and choose $\psi = (\nabla \cdot U)/k^2$; then the appropriate Helmholtz equation is

$$\nabla^2 \vec{U} + k^2 \vec{U} = -4\pi i \frac{\mu\omega}{C^2} \tilde{\vec{J}}_o \tag{50}$$

with the formal solution

$$\vec{U} = i \tilde{Z} k \iiint_{V'} \vec{J}_o (\vec{r}\,') G (\vec{r}, \vec{r}\,') d^3 \vec{r}\,' \tag{51}$$

where Z is the wave impedance defined in Eq. (12) and

$$G(\vec{r}, \vec{r}\,') = \frac{e^{ik|r - r'|}}{4\pi |r - r'|}$$

*The author acknowledges Dr. C. M. Butler of the University of Mississippi for bringing this point to his attention. Dr. Butler also supplied a derivation of the coupled integral differential equations based on vector and scalar potentials.

is a Green's function which has an integrable singularity at $\vec{r} = \vec{r}'$, and $\vec{r}'$ and $\vec{r}$ are, respectively, vectors from the origin to a current element and to the observation point (r, θ, ϕ).

It is convenient, at this point, to state the radial unit vector of a source point in terms of the coordinates of the observation point for both spherical and cylindrical coordinate systems (see Fig. 2). For a source point on the surface of either cone, we find

$$\hat{r}' = \hat{\rho} \sin\theta' \cos(\phi - \phi') + \hat{z} \cos\theta' - \hat{\phi} \sin(\phi - \phi') \sin\theta' \tag{52}$$

and

$$\hat{r}' = \hat{r}[\sin\theta' \sin\theta \cos(\phi - \phi') + \cos\theta' \cos\theta]$$

$$+ \hat{\theta}[\sin\theta' \cos\theta \cos(\phi - \phi') - \cos\theta' \sin\theta] - \hat{\phi} \sin\theta' \sin(\phi - \phi') \tag{53}$$

with

$$\theta' = \theta_c, \pi - \theta_c$$

Similarly, for a source point on the surface of either end cap, we find

$$\hat{\rho}' = \hat{\rho} \cos(\phi - \phi') - \hat{\phi} \sin(\phi - \phi') \tag{54}$$

and

$$\hat{\rho}' = \hat{r} \sin\theta \cos(\phi - \phi') + \hat{\theta} \cos\theta \cos(\phi - \phi') - \hat{\phi} \sin(\phi - \phi') \tag{55}$$

with

$$z' = \pm h$$

These projections will be used to determine the magnitude of the vector, $r - \vec{r}'$, from source point to observation point for four specific cases and the associated Green's functions.

The Green's function for current elements and observation point both on the conical surfaces is now stated as

$$G_{bc}^{1}(\vec{r}, \vec{r}') = \frac{e^{ikR_1}}{4\pi R_1}$$

with

$$R_1 = \Big|_{\theta' \to \theta_c, \pi - \theta_c} \sqrt{r^2 + r'^2 - 2rr'[\sin\theta \sin\theta' \cos(\phi - \phi') + \cos\theta \cos\theta']} \tag{56}$$

The Green's function for current elements on the end caps and observation point on the conical surfaces is

$$G^2_{cp}(\vec{r}, \vec{r}\,') = \frac{e^{ik R_2}}{4\pi R_2}$$

with

$$R_2 = \left| \sqrt{r^2 + z'^2 + \rho'^2 - 2r(\sin\theta\rho'\cos(\phi - \phi') + z'\cos\theta)} \right|_{z' \to \pm h} \tag{57}$$

The Green's function for current elements and observation point both on the end caps is

$$G^1_{cp}(\vec{r}, \vec{r}\,') = \frac{e^{ik\rho_1}}{4\pi\rho_1}$$

with

$$\rho_1 = \left| \sqrt{\rho^2 + z^2 + \rho'^2 + z'^2 - 2[\rho\rho'\cos(\phi - \phi') + z\,z']} \right|_{z' \to \pm h} \tag{58}$$

Finally, the Green's function for current elements on the conical surfaces and observation point on the end caps is

$$G^2_{bc}(\vec{r}, \vec{r}\,') = \frac{e^{ik\rho_2}}{\rho_2}$$

with

$$\rho_2 = \left| \sqrt{\rho^2 + z^2 + r'^2 - 2r'[\sin\theta'\rho\cos(\phi - \phi') + z\cos\theta']} \right|_{\theta' \to \theta_c,\ \pi - \theta_c} \tag{59}$$

Having constructed the Green's function for the four cases of interest, we may now determine the current flowing in the conical surfaces and in the end caps. The conical source is a loop of current flowing in the (outward or inward) radial direction whose magnitude is given by

$$\tilde{I}_{bc}(r') = 2\pi \sin\theta_c\, t_{bc}\, \vec{r}\,' \cdot \tilde{\vec{J}}^{bc}_o(\vec{r}\,') \tag{60}$$

where t_{bc} is the thickness of the very thin surface layer in which current flow occurs. In obtaining Eq. (43), we have used the approximation that

$$\int_{\theta_c - (\Delta\theta'/2)}^{\theta_c + (\Delta\theta'/2)} \sin\theta' \, d\theta' = \sin\theta_c \frac{t_{bc}}{r'}$$

with

$$\Delta\theta' = \frac{t_{bc}}{r'}$$

The volume element is, similarly, reduced to

$$d^3\vec{r}\,' = r' t_{bc} \sin\theta_c \left\{ \delta(\theta' - \theta_c), \delta\left[\theta' - (\pi - \theta_c)\right] \right\} d\theta' \, d\phi' \, dr'$$

Allowing for the phase difference between currents flowing in the two cones, we obtain, finally,

$$\tilde{\vec{J}}_o^{bc}(\vec{r}\,') \, d^3\vec{r}\,' = \hat{r}' \tilde{I}_{bc}(r') \left\{ \delta(\theta' - \theta_c) - \delta\left[\theta' - (\pi - \theta_c)\right] \right\} dr' \, d\theta' \frac{d\phi'}{2\pi} \tag{61}$$

By analogous reasoning, we find the cap current density volume element product to be

$$\tilde{\vec{J}}_o^{cp}(\vec{r}\,') \, d^3\vec{r}\,' = \hat{\rho}' I_{cp}(\rho) \left[\delta(z' - h) - \delta(z' + h) \right] d\rho' \, dz' \frac{d\phi'}{2\pi} \tag{62}$$

with

$$I_{cp}(\rho = 0) = 0$$

The contribution of both cone currents and cap currents to the auxiliary function $\vec{U}$, evaluated near a cone, is found [from Eqs. (51), (61), and (62)] to be

$$\vec{U}_{bc} = i\tilde{Z}k \left\{ \int_o^{2\pi} \int_\delta^d \hat{r}' \tilde{I}_{bc}(r') \left[\chi_{bc}^{1+}(\vec{r}, r', \phi') - \chi_{bc}^{1-}(\vec{r}, r', \phi') \right] dr' \frac{d\phi'}{2\pi} \right.$$

$$\left. + \int_o^{2\pi} \int_o^{\rho_o} \hat{\rho}' \tilde{I}_{cp}(\rho') \left[\chi_{cp}^{2+}(\vec{r}, \rho', \phi') - \chi_{cp}^{2-}(\vec{r}, \rho', \phi') \right] d\rho' \frac{d\phi'}{2\pi} \right\} \tag{63}$$

where

$$\chi^{1}_{bc}\ (\vec{r},\ r',\ \phi') \equiv \int_{\theta_c - (\Delta\theta'/2)}^{\theta_c + (\Delta\theta'/2)} G^{1}_{bc}\ (\vec{r},\ \vec{r}')\ \left[\delta(\theta' - \theta_c),\ \delta(\theta' - (\pi - \theta_c))\right]\ d\theta'$$

and

$$\chi^{2\,\pm}_{cp}(\vec{r},\ \rho',\ \phi') \equiv \int_{\pm\,[\,h - (t_{cp}/2)\,]}^{\pm\,[\,h + (t_{cp}/2)\,]} G^{2}_{cp}\ (\vec{r},\ \vec{r}')\ \left[\delta(Z' - h),\ \delta(Z' + h)\right] dZ'$$

where t_{cp} is the thickness of the current-carrying layer in the end cap surfaces.

Similarly, the form of $\vec{U}$ evaluated near a cap is

$$\vec{U}_{cp} = i\tilde{Z}k\left\{\int_0^{2\pi}\int_{\delta}^{d} \hat{r}'\,\tilde{I}_{bc}(r')\left[\chi^{2+}_{bc}(\vec{r},\ r',\ \phi') - \chi^{2-}_{bc}\ (\vec{r},\ r',\ \phi')\right] dr'\ \frac{d\phi'}{2\pi}\right.$$

$$\left. + \int_0^{2\pi}\int_0^{\rho_0} \hat{\rho}'\,\tilde{I}_{cp}(\rho')\left[\chi^{1+}_{cp}(\vec{r},\ \rho',\ \phi') - \chi^{1-}_{cp}\ (\vec{r},\ \rho',\ \phi')\right] d\rho'\ \frac{d\phi'}{2\pi}\right\} \tag{64}$$

where

$$\chi^{2\,\pm}_{bc}(\vec{r},\ r',\ \phi') \equiv \int_{\theta_c - \frac{\Delta\theta'}{2}}^{\theta_c + \frac{\Delta\theta'}{2}} G^{2}_{bc}\ (\vec{r},\ \vec{r}')\ \left[\delta(\theta' - \theta_c),\ \delta(\theta' - (\pi - \theta_c))\right]\ d\theta' \tag{64a}$$

and

$$\chi^{1\,\pm}_{cp}(\vec{r},\ \rho',\ \phi') \equiv \int_{\pm\ h - \frac{t_{cp}}{2}}^{\pm\ \ h + \frac{t_{cp}}{2}} G^{1}_{cp}\ (\vec{r},\ \vec{r}')\left[\delta(Z' - h),\ \delta(Z' + h)\right] d\theta' \tag{64b}$$

In forming the divergences of these functions, we note that the gradient operates, initially, only on the unprimed coordinates in the Green's functions. Thus, the divergences have the form

$$\nabla \cdot U = i\tilde{Z}k \int_0^{2\pi} \int_a^b \tilde{I}(n')\, \hat{n}' \cdot \vec{\nabla}\, \chi^{\pm}(\vec{r}, n', \phi')\, dn' \frac{d\phi'}{2\pi}$$

$$= i\tilde{Z}k \int_0^{2\pi} \int_a^b \tilde{I}(n') \frac{\partial \chi^{\pm}}{\partial n'}(\vec{r}, n', \phi')\, dn' \frac{d\phi'}{2\pi} \tag{65}$$

where $\hat{n}'$ is the unit vector in the direction of current flow and n' is the associated coordinate.

The latter form can be integrated by parts, yielding

$$\nabla \cdot U = i\tilde{Z}k \left\{ \tilde{I}(n') \int_0^{2\pi} \chi^{\mp}(\vec{r}, n', \phi') \frac{d\phi'}{2\pi} \Big]_{n'=a}^{n'=b} - \int_a^b \frac{\partial I(n')}{\partial n'} \int_0^{2\pi} \chi^{\mp}(\vec{r}, n', \phi') \frac{d\phi'}{2\pi} dn' \right\} \tag{66}$$

In an ordinary boundary value problem, the Green's function would normally be defined so as to assure vanishing of integrated parts containing either the current (Dirichlet boundary conditions) or its normal derivative (Neumann boundary conditions) on the surface enclosing the source elements. In this case, however, the boundary conditions which must be satisfied are the vanishing of the tangential fields at the surfaces and the Kirchoff's law for continuity of current at the cone-cap junctures. The latter is stated as

$$\tilde{I}_{cp}(\rho_c) + \tilde{I}_{bc}(d) \equiv 0 \tag{67}$$

Since it can be shown that $\chi^{2\pm}_{cp}(r, \rho_o, \phi') = \chi^{1\pm}_{bc}(r, d, \phi')$, one can write the divergence of the auxiliary function near the conical surfaces [incorporating Eq. (67) into Eq. (66)] as

$$\nabla \cdot U_{bc}(\vec{r}) = -i\tilde{Z}k \left\{ \tilde{I}_{bc}(\delta) \int_0^{2\pi} \left[\chi^{1+}_{bc}(\vec{r}, \delta, \phi') - \chi^{1-}_{bc}(\vec{r}, \delta, \phi') \right] \frac{d\phi'}{2\pi} \right.$$

$$+ \int_0^{\rho_o} \frac{\partial \tilde{I}_{cp}(\rho')}{\partial \rho'} \int_0^{2\pi} \left[\chi^{2+}_{cp}(\vec{r}, \rho', \phi') - \chi^{2-}_{cp}(\vec{r}, \rho', \phi') \right] \frac{d\phi'}{2\pi} d\rho'$$

$$\left. + \int_\delta^d \frac{\partial \tilde{I}_{bc}(r')}{\partial r'} \int_0^{2\pi} \left[\chi^{1-}_{bc}(\vec{r}, r', \phi') - \chi^{1-}(\vec{r}, r', \phi') \right] \frac{d\phi'}{2\pi} dr' \right\} \tag{68}$$

Again, through an analogous reasoning process, we obtain

$$\nabla \cdot \vec{U}_{cp}(\vec{r}) = -i\tilde{Y}k\left\{\tilde{I}_{bc}(\delta)\int_0^{2\pi}\left[\chi_{bc}^{2+}(\vec{r},\delta,\phi') - \chi_{bc}^{2-}(\vec{r},\delta,\phi')\right]\frac{d\phi'}{2\pi}\right.$$

$$\mp\int_0^{\rho_0}\frac{\partial\tilde{I}_{cp}(\rho')}{\partial\rho'}\int_0^{2\pi}\left[\chi_{cp}^{1\mp}(\vec{r},\rho',\phi') - \chi_{cp}^{1-}(\vec{r},\rho',\phi')\right]\frac{d\phi'}{2\pi}\,d\rho'$$

$$\left.-\int_\delta^d\frac{\partial\tilde{I}_{bc}(r')}{\partial r'}\int_0^{2\pi}\left[\chi_{bc}^{2+}(\vec{r},r',\phi') - \chi_{bc}^{2-}(\vec{r},r',\phi')\right]\frac{d\phi'}{2\pi}\,dr'\right\} \tag{69}$$

These divergences act as scalar potentials, as can be seen from Eq. (49).

The final expressions for the tangential fields are obtained from Eqs. (49), (63), (64), (68), and (69), using the following cross products:

$$\hat{\theta}\times\hat{r}' = -\hat{\phi}\,[\sin\theta'\sin\theta\cos(\phi-\phi') + \cos\theta'\cos\theta] - \hat{r}\sin\theta'\sin(\phi-\phi')$$

$$\hat{\theta}\times\hat{\rho}' = -\hat{\phi}\sin\theta\cos(\phi-\phi') - \hat{r}\sin(\phi-\phi')$$

$$\hat{\theta}\times\vec{\nabla} = -\hat{\phi}\frac{\partial}{\partial r} - \frac{\hat{r}}{r\sin\theta}\frac{\partial}{\partial\phi}$$

$$\hat{z}\times\hat{r}' = \hat{\phi}\sin\theta'\cos(\phi-\phi') + \hat{\rho}\sin\theta'\sin(\phi-\phi')$$

$$z\times\hat{\rho}' = \hat{\phi}\cos(\phi-\phi') + \hat{\rho}\sin(\phi-\phi')$$

$$\hat{z}\times\vec{\nabla} = \hat{\phi}\frac{\partial}{\partial\rho} + \frac{\hat{\rho}}{\rho}\frac{\partial}{\partial\phi} \tag{70}$$

which were obtained from Eqs. (35) through (38). When Eq. (70) is used to obtain the tangential field components from Eqs. (49), (63), (64), (68), and (69), the terms proportional to $\sin(\phi-\phi')$ do not survive integration, since these are odd terms, whereas all other terms in the integrands having the form of Eq. (70) are even terms. In addition, the aximuthal derivatives vanish by symmetry. Thus, the tangential electric fields are purely azimuthal, both near the cones and near the caps.

It is convenient to introduce three classes of kernel functions defined as follows:

$$\mathcal{K}(\vec{r}, n') = \int_0^{2\pi} [\chi^+(\vec{r}, n', \phi') - \chi^-(\vec{r}, n', \phi')] \frac{d\phi'}{2\pi}$$

$$\mathcal{L}(\vec{r}, n') = \int_0^{2\pi} \cos\phi' [\chi^+(\vec{r}, n', \phi') - \chi^-(\vec{r}, n', \phi')] \frac{d\phi'}{2\pi}$$

$$\mathcal{M}(\vec{r}, n') = \int_0^{2\pi} [\chi^+(\vec{r}, n', \phi') - \chi^-(\vec{r}, n', \phi')] \frac{d\phi'}{2\pi} \tag{71}$$

We state the final field equations, in terms of these functions, noting that cylindrical symmetry permits ϕ' to be set equal to zero and with the order of integration interchanged.

$$\hat{\theta} \times \tilde{\vec{E}}_{bc} = -i\hat{\phi}\tilde{Z}k\Bigg\{\sin\theta_c \sin\theta \int_\delta^d \tilde{I}_{bc}(r')\mathcal{L}^1_{bc}(\vec{r}, r')\,dr' + \cos\theta_c \cos\theta \int_\delta^d \tilde{I}_{bc}(r')\mathcal{M}^1(\vec{r}, r')\,dr'$$

$$+ \sin\theta_c \int_0^{\rho_o} \tilde{I}_{cp}(\rho')\mathcal{K}^2_{cp}(\vec{r}, \rho')\,d\rho' - \Bigg[\tilde{I}_{bc}(\delta)\frac{\partial}{\partial r}\mathcal{K}^1_{bc}(\vec{r}, \delta)$$

$$+ \frac{\partial}{\partial r}\int_\delta^d \frac{d\tilde{I}_{bc}(r')}{dr'}\mathcal{K}^1_{bc}(\vec{r}, r')\,dr' + \frac{\partial}{\partial r}\int_0^{\rho_o} \frac{d\tilde{I}_{cp}(\rho')}{d\rho'}\mathcal{K}^2_{cp}(\vec{r}, \rho')\,d\rho'\Bigg]\Bigg\} \tag{72}$$

and

$$\hat{z} \times \tilde{\vec{E}}_{bc} = i\hat{\phi}\tilde{Z}k\Bigg\{\sin\theta_c \int_\delta^d \tilde{I}_{bc}(r')\mathcal{L}^2_{bc}(\vec{r}, r')\,dr' + \int_0^{\rho_o} \tilde{I}_{cp}(\rho')\mathcal{L}^1_{cp}(\vec{r}, \rho')\,d\rho'$$

$$- \Bigg[\tilde{I}_{bc}(\delta)\frac{\partial}{\partial\rho}\mathcal{K}^2_{bc}(\vec{r}, \delta) + \frac{\partial}{\partial\rho}\int_\delta^d \frac{d\tilde{I}_{bc}(r')}{dr'}\mathcal{K}^2_{bc}(\vec{r}, r')\,dr'$$

$$+ \frac{\partial}{\partial\rho}\int_0^{\rho_o} \frac{d\tilde{I}_{cp}(\rho')}{d\rho'}\mathcal{K}^1_{cp}(\vec{r}, \rho')\,d\rho'\Bigg]\Bigg\} \tag{73}$$

The coupled integrodifferential equations for the currents, I_{bc}, on the cones and I_{cp} on the caps, are obtained by setting Eqs. (72) and (73) equal to zero in the limits $\theta \to \theta_c$, $\pi - \theta_c$, and $z \to \pm h$. The results are stated as follows:

$$0 = \sin^2\theta_c \int_\delta^d \tilde{I}_{bc}(r')\,\mathfrak{L}^1_{bc}(\vec{r}, r')\,dr' + \cos^2\theta_c \cos\theta \int_\delta^d \tilde{I}_{bc}(r')\,\mathfrak{M}^1(\vec{r}, r')\,dr'$$

$$+ \sin\theta_c \int_o^{\rho_o} \tilde{I}_{cp}(\rho')\,K^2_{cp}(\vec{r}, \rho')\,d\rho' - \left[\tilde{I}_{bc}(\delta)\frac{\partial}{\partial r}K^1_{bc}(\vec{r}, \delta)\right.$$

$$\left. + \frac{\partial}{\partial r}\left(\int_\delta^d \frac{d\tilde{I}_{bc}(r')}{dr'}K^1_{bc}(\vec{r}, r')\,dr'\right) + \frac{\partial}{\partial r}\left(\int_o^{\rho_o}\frac{d\tilde{I}_{cp}(\rho')}{d\rho'}K^2_{cp}(\vec{r}, \rho')\,d\rho'\right)\right] \tag{74}$$

and

$$\sin\theta_c \int_\delta^d \tilde{I}_{bc}(r')\,\mathfrak{L}^2_{bc}(\vec{r}, r')\,dr' + \int_o^{\rho_o}\tilde{I}_{cp}(\rho')\,\mathfrak{L}^1_{cp}(\vec{r}, \rho')\,d\rho'$$

$$- \left[\tilde{I}_{bc}(\delta)\frac{\partial}{\partial\rho}K^2_{bc}(\vec{r}, \delta)\right.$$

$$\left. + \frac{\partial}{\partial r}\left(\int_\delta^d \frac{d\tilde{I}_{bc}(r')}{dr'}K^2_{bc}(\vec{r}, r')\,dr'\right) + \frac{\partial}{\partial\rho}\left(\int_o^{\rho_o}\frac{d\tilde{I}_{cp}(\rho')}{d\rho'}K^1_{cp}(\vec{r}, \rho')\,d\rho'\right)\right] = 0 \tag{75}$$

In using these equations, note that $\vec{r} = (\hat{\varrho}\varrho) + (\hat{z}\,z)$, in order to evaluate terms in $\partial/\partial\varrho$.

There are several options for solving these equations. Conventionally, the method of moments (Ref. 8) can be used to reduce the equations to a system of algebraic equations, provided that the singularities in the kernels $\ddot{K}$, $\mathfrak{L}$, and $\mathfrak{M}$ can be isolated. This method involves establishing a computational mesh on both the cone surfaces and on the end caps. The currents are expanded in a series of functions chosen for computational convenience and defined within each interval of the mesh. Weighting functions (known as testing functions) are similarly chosen, and the expanded Eqs. (74) and (75) are premultiplied by these functions. Integrating the resulting equations over the finite elements of the computational mesh then yields algebraic relations for the current expansion coefficients which can be solved by matrix methods. A large body of literature exists that centers on this method and the properties of various expansion and testing functions (in the context of specific functions) (e.g., Refs. 9 through 11). When the expansion and testing functions are the same, the procedure is known as Galerkin's method (e.g., Ref. 12). In view of the physical significance of sinusoidal currents demonstrated in Section 3.2.1, it is appealing to use piecewise sinusoidal functions as either or both expansion or testing functions, provided that the resulting integrals are evaluable. It should be noted, however, that simpler functions have been found useful (Ref. 10), although a finer mesh may be required. Further discussion of the method of moments is beyond the scope of this report. It may be possible to devise a

simpler scheme to solve Eqs. (74) and (75). Regardless of how the solution is effected, the resultant current distribution must then be inserted into Eq. (39) to obtain the source multipole coefficients for the biconical antenna. If the method of moments is used, then, obviously, the expansion functions should be chosen with ease of integration of Eq. (39) in mind.

3.3 FORMULATION OF THE CAVITY BOUNDARY VALUE PROBLEM

In this section the multipole expansion for the Hertz-Debye potentials is obtained for all regions of the spherical cavity external to the source. For simplicity, the surface of the sphere is assumed to be much thicker than its skin depth at all frequencies of interest. The multipole coefficients in each region of the cavity (see Figs. 3 and 5) are then obtained by applying the boundary conditions stated in Eq. (29) to the potential expansion shown in Eq. (32). We illustrate the procedure by deriving the multipole coefficients, first, for an empty sphere and comparing our results, in the limit of a Hertzian dipole source, with those of Ref. 13. After this discussion, the matrix formulation for N dampers is presented, and the results for one and two dampers are derived in detail. Throughout this section the full expansion corresponding to an arbitrary source distribution [Eqs. (37) and (38)] will be retained, rather than assuming source axisymmetry. The following notation convention will be employed:

1. Capital English letters denote coefficients of standing waves (Ricatti-Bessel functions with real arguments).

2. Lower-case English letters denote coefficients of outwardly propagating (plus left superscript) or inwardly propagating (minus left superscript) undamped spherical waves (Ricatti-Hänkel functions of the first and second kind, respectively, with real arguments).

3. Greek letters denote coefficients of outwardly propagating (plus left superscript) or inwardly propagating (minus left superscript) damped spherical waves (Ricatti-Hänkel functions with complex arguments).

To illustrate this convention, in reference to Fig. 3, the multipole coefficients for the single damper configuration are related to the corresponding spatial regions as follows:

a. Source region - ${}_{\ell}^{m}a$, ${}_{\ell}^{m}b$

b. Region I - between source and damper - ${}_{\ell}^{m}A$, ${}_{\ell}^{m}B$

c. Region II - damper - ${}^{\pm}{}_{\ell}^{m}\alpha$, ${}^{\pm}{}_{\ell}^{m}\beta$

d. Region III - between damper and surface - E_ℓ^m, M_ℓ^m ; $^-e_\ell^m$, $^-m_\ell^m$

e. Surface region - $^+\gamma_\ell^m$, $^+\delta_\ell^m$

Note that the first of each pair of coefficients denotes the TM wave multipole coefficient and the second denotes the TE wave multipole coefficient. We shall return to the single damper problem later, but now we shall consider the empty cavity problem to illustrate the formulation and solution of the boundary value problem relating all other multipole coefficients to the source multipoles a_ℓ^m and b_ℓ^m, whose relationships to the source current distribution have been stated in Eqs. (37) and (38).

3.3.1 Multipole Expansion Coefficients for an Empty Cavity

From Eqs. (29) and (30) we obtain the relations between inerior and exterior solutions* for the TM waves in a cavity containing a nondissipative medium:

$$\beta_s \frac{\epsilon}{\epsilon_s}\left[a_\ell^m \zeta_\ell^1(\alpha_s) + A_\ell^m \psi_\ell(\alpha_s)\right] = {}^+\gamma_\ell^m \zeta_\ell^1(\beta_s \alpha_s)$$

and

$$\frac{a_\ell^m \zeta_\ell^{1'}(\alpha_s) + A_\ell^m \psi_\ell'(\alpha_s)}{1 + \frac{4\pi\sigma i}{\epsilon\omega}} = \frac{{}^+\gamma_\ell^m \zeta_\ell^{1'}(\beta_s \alpha_s)}{\left(1 + \frac{4\pi\sigma i}{\epsilon\omega}\right)_s} \tag{76}$$

where the subscript "s" denotes surface, $\alpha_s = k_o R$, $\beta_s = k_s/k_o$, and the ratio of interior and surface impedances is $Z/Z_s = \beta_s(\mu/\mu_s)$, with

$$\frac{\omega}{c}\mu_s \epsilon_s \left[\left(1 + \frac{4\pi\sigma_s i}{\epsilon_s \omega}\right)\right]^{1/2} \simeq \frac{1+i}{\delta_s}$$

The corresponding equations for TE waves are

$$\beta_s \frac{\mu}{\mu_s}\left[b_\ell^m \zeta_\ell^1(\alpha_s) + B_\ell^m \psi_\ell(\alpha_s)\right] = {}^+\delta_\ell^m \zeta_\ell^1(\beta_s \alpha_s)$$

and

$$b_\ell^m \zeta_\ell^{1'}(\alpha_s) + B_\ell^m \psi_\ell'(\alpha_s) = {}^+\delta_\ell^m \zeta_\ell^{1'}(\beta_s \alpha_s) \tag{77}$$

*Henceforth, primes denote differentiation of a function with respect to its argument.

Eliminating the surface multipole coefficients, ${}^{+}\gamma_\ell^m$ and ${}^{+}\delta_\ell^m$, from these equations produces the cavity multipole coefficients (i.e., the coefficients of standing waves in the cavity) for both the TM and TE waves

$$A_\ell^m = a_\ell^m \left\{ \frac{\beta_s \frac{\mu}{\mu_s} \zeta_\ell^{1\prime}(a_s)\zeta_\ell^1(\beta_s a_s) - \zeta_\ell^1(a_s)\zeta_\ell^{1\prime}(\beta_s a_s)}{\psi_\ell(a_s)\zeta_\ell^{1\prime}(\beta_s a_s) - \beta_s \frac{\mu}{\mu_s}\zeta_\ell^1(\beta_s a_s)\psi_\ell'(a_s)} \right\} \tag{78}$$

and

$$B_\ell^m = b_\ell^m \left\{ \frac{\beta_s \frac{\mu}{\mu_s} \zeta_\ell^1(a_s)\zeta_\ell^{1\prime}(\beta_s a_s) - \zeta_\ell^{1\prime}(a_s)\zeta_\ell^1(\beta_s a_s)}{\psi_\ell'(a_s)\zeta_\ell^1(\beta_s a_s) - \beta_s \frac{\mu}{\mu_s}\zeta_\ell^{1\prime}(\beta_s a_s)\psi_\ell(a_s)} \right\} \tag{79}$$

These standing wave coefficients have an obvious similarity to the well known Mie-scattering coefficients—except that here the problem is one of an empty cavity surrounded by an electrically infinite, absorbing medium, whereas the usual Mie-scattering problem is one of an absorbing and dispersive sphere embedded in a nonabsorptive medium. These coefficients are now used to obtain the cavity fields for comparison with an earlier analysis.

In an early study, Butler and Van Bladel (Ref. 13) obtained the fields inside a dipole-excited hollow sphere embedded in an infinite dielectric medium. To compare our results with theirs, we form the ratio of the tangential electric and magnetic fields at the inner surface of the sphere:

$$\frac{E_\theta}{H_\phi} = \frac{k_s C}{i\bar{\epsilon}_s \omega} \left(\frac{\partial^2 \alpha \pi_E}{\partial \alpha \, \partial \theta} \Big/ \frac{\partial \alpha \pi_E}{\partial \theta} \right)_s \tag{80}$$

since the azimuthal derivatives in Eqs. (27) and (28) vanish because of axisymmetry. For a small dipole, $|kd| << 1$, only the first multipole is important, and, using

$$\zeta_\ell^1(a_s) = a_s h_\ell^1(a_s) \text{ and } k_s = \sqrt{\mu_s \epsilon_s}\,\frac{\omega}{C}\left(1 + \frac{4\pi\sigma i}{\epsilon\omega}\right)_s^{1/2}$$

we obtain

$$\frac{E_\theta}{H_\phi} = -\frac{iC}{\bar{\epsilon}_s \omega R}\left[\frac{h_1^1(a_s) + a_s h_1^{1\prime}(a_s)}{h_1^1(a_s)}\right]$$

where

$$\bar{\epsilon}_s = \epsilon_s\left(1 - \frac{4\pi\sigma i}{\epsilon\omega}\right)_s \tag{81}$$

This is the result obtained by Butler and Van Bladel (Ref. 13). Note that our choice of the sign of ω [from Eq. (5)] dictates the use of $h_\lambda^{(1)}(\alpha_s)$ for correct outgoing boundary conditions, whereas Butler and Van Bladel use the opposite sign for ω and, hence $h_\lambda^{(2)}(\alpha_s)$ for outgoing waves. Also, our use of Gaussian units introduces a factor C into Eq. (81), in contrast to Butler and Van Bladel's form of Eq. (83).

3.3.2 Matrix Formulation for the multipole Coefficients for the Multipole Coefficients in a Cavity Containing N Dampers

The most systematic way of incorporating the boundary conditions stated in Eq. (29) into the boundary value problem for a cavity containing several dampers is to use matrix procedures. Let us define the source column vectors, whose dimensions are 2(2N + 1), $\underline{Y}_E$ and $\underline{Y}_M$, as vectors whose first elements are proportional to a_ℓ^m and b_ℓ^m, respectively, and whose remaining elements are all zero. The column vectors for the unknown multipole coefficients are denoted, accordingly, as $\underline{X}_E$ and $\underline{X}_M$. These vectors are obtained by inversion of the matrix equations

$$\underline{\underline{M}}^E \, \underline{X}_E = \underline{Y}_E \text{ and } \underline{\underline{M}}^M \, \underline{X}_M = \underline{Y}_M \tag{82}$$

where the matrices $\underline{\underline{M}}^E$ and $\underline{\underline{M}}^M$ are interface matrices for TM and TE waves, respectively. In accordance with the notation given in Section 3.3, the vectors of unknown multipole coefficients have the following form:

$$\underline{X}_E^T = \left(\left(A_\ell^m, \; {}^{+}a_{1,\ell}^m, \; {}^{-}a_{1,\ell}^m, \; {}^{+}c_{1,\ell}^m, \; {}^{-}c_{1,\ell}^m, \; {}^{+}a_{2,\ell}^m, \; {}^{-}a_{2,\ell}^m, \; {}^{+}c_{2,\ell}^m, \; {}^{-}c_{2,\ell}^m, \cdots \right. \right.$$
$$\left. \left. {}^{+}a_{N,\ell}^m, \; {}^{-}a_{N,\ell}^m, \; {}^{-}e_\ell^m, \; E_\ell^m, \; {}^{-}\gamma_\ell^m \right) \right)$$

$$\underline{X}_M^T = \left(\left(B_\ell^m, \; {}^{+}\beta_{1,\ell}^m, \; {}^{-}\beta_{1,\ell}^m, \; {}^{+}d_{1,\ell}^m, \; {}^{-}d_{1,\ell}^m, \; {}^{+}\beta_{2,\ell}^m, \; {}^{-}\beta_{2,\ell}^m, \; {}^{+}d_{2,\ell}^m, \; {}^{-}d_{2,\ell}^m, \cdots \right. \right.$$
$$\left. \left. {}^{+}\beta_{N,\ell}^m, \; {}^{-}\beta_{N,\ell}^m, \; {}^{-}m_\ell^m, \; M_\ell^m, \; {}^{+}\delta_\ell^m \right) \right) \tag{83}$$

where $\underline{X}^T$ denotes transpose of the vector.

It should be recalled that there are 2 x (2N + 1) elements in each of these vectors. The form of the interface matrices is shown, schematically, in Fig. 4. For TM waves, the rectangular submatrices in the interface matrix have the following form:

$$M_o^E = \begin{pmatrix} \beta_{D_1} \frac{\epsilon}{\bar{\epsilon}_{D_1}} \psi_\ell(a_o) \\ \beta_{D_1}^2 \frac{\epsilon}{\bar{\epsilon}_{D_1}} \frac{\mu}{\mu_{D_1}} \psi_\ell'(a_o) \end{pmatrix} \tag{84a}$$

$$M_{D_j}^E = \begin{pmatrix} -\zeta_\ell^1\left(\beta_{D_j} a_{2j-2}\right) & -\zeta_\ell^2\left(\beta_{D_j} a_{2j-2}\right) \\ -\zeta_\ell^{1\prime}\left(\beta_{D_j} a_{2j-2}\right) & -\zeta_\ell^{2\prime}\left(\beta_{D_j} a_{2j-2}\right) \\ \zeta_\ell^1\left(\beta_{D_j} a_{2j-1}\right) & \zeta_\ell^2\left(\beta_{D_j} a_{2j-1}\right) \\ \zeta_\ell^{1\prime}\left(\beta_{D_j} a_{2j-1}\right) & \zeta_\ell^{2\prime}\left(\beta_{D_j} a_{2j-1}\right) \end{pmatrix} \tag{84b}$$

$$M_{int_j}^E = \begin{pmatrix} -\beta_{D_j} \frac{\epsilon}{\bar{\epsilon}_{D_j}} \zeta_\ell^1\left(a_{2j-1}\right) & -\beta_{D_j} \frac{\epsilon}{\bar{\epsilon}_{D_j}} \zeta_\ell^2\left(a_{2j-1}\right) \\ -\beta_{D_j}^2 \frac{\epsilon}{\bar{\epsilon}_{D_j}} \frac{\mu}{\mu_{D_j}} \zeta_\ell^{1\prime}\left(\beta_{D_j} a_{2j-1}\right) & -\beta_{D_j}^2 \frac{\epsilon}{\bar{\epsilon}_{D_j}} \frac{\mu}{\mu_{D_j}} \zeta_\ell^{2\prime}\left(\beta_{D_j} a_{2j-1}\right) \\ \beta_{D_j} \frac{\epsilon}{\bar{\epsilon}_{D_j}} \zeta_\ell^1\left(a_{2j}\right) & \beta_{D_j} \frac{\epsilon}{\bar{\epsilon}_{D_j}} \zeta_\ell^2\left(a_{2j}\right) \\ \beta_{D_j}^2 \frac{\epsilon}{\bar{\epsilon}_{D_j}} \frac{\mu}{\mu_{D_j}} \zeta_\ell^{1\prime}\left(a_{2j}\right) & \beta_{D_j}^2 \frac{\epsilon}{\bar{\epsilon}_{D_j}} \frac{\mu}{\mu_{D_j}} \zeta_\ell^{2\prime}\left(a_{2j}\right) \end{pmatrix} \tag{84c}$$

$$M_{ex}^E = \begin{pmatrix} -\beta_{D_N} \frac{\epsilon}{\bar{\epsilon}_{D_N}} \zeta_\ell^1\left(a_{2N}\right) & -\beta_{D_N} \frac{\epsilon}{\bar{\epsilon}_{D_N}} \psi_\ell\left(a_{2N}\right) \\ -\beta_{D_N}^2 \frac{\epsilon}{\bar{\epsilon}_{D_N}} \frac{\mu}{\mu_{D_N}} \zeta_\ell^{2\prime}\left(a_{2N}\right) & -\beta_{D_N}^2 \frac{\epsilon}{\bar{\epsilon}_{D_N}} \frac{\mu}{\mu_{D_N}} \psi_\ell'\left(a_{2N}\right) \\ \beta_s \frac{\epsilon}{\bar{\epsilon}_s} \zeta_\ell^2\left(a_{2N+1}\right) & \beta_s \frac{\epsilon}{\bar{\epsilon}_s} \psi_\ell\left(a_{2N+1}\right) \\ \beta_s^2 \frac{\epsilon}{\bar{\epsilon}_s} \frac{\mu}{\mu_s} \zeta_\ell^{2\prime}\left(a_{2N+1}\right) & \beta_s^2 \frac{\epsilon}{\bar{\epsilon}_s} \frac{\mu}{\mu_s} \psi_\ell'\left(a_{2N+1}\right) \end{pmatrix} \tag{84d}$$

$$M_S^E = \begin{pmatrix} -\zeta_\ell^1 \left(\beta_s \alpha_{2N+1}\right) \\ -\zeta_\ell^{1'} \left(\beta_s \alpha_{2N+1}\right) \end{pmatrix} \tag{84e}$$

where

$$\alpha_o = k_o r_a$$

$$\alpha_1 = k_o r_b$$

$$\cdots$$

$$\alpha_{2N+1} = k_o R = \alpha_s$$

and

$$\beta_{D_j} = \frac{k_{D_j}}{k_o}$$

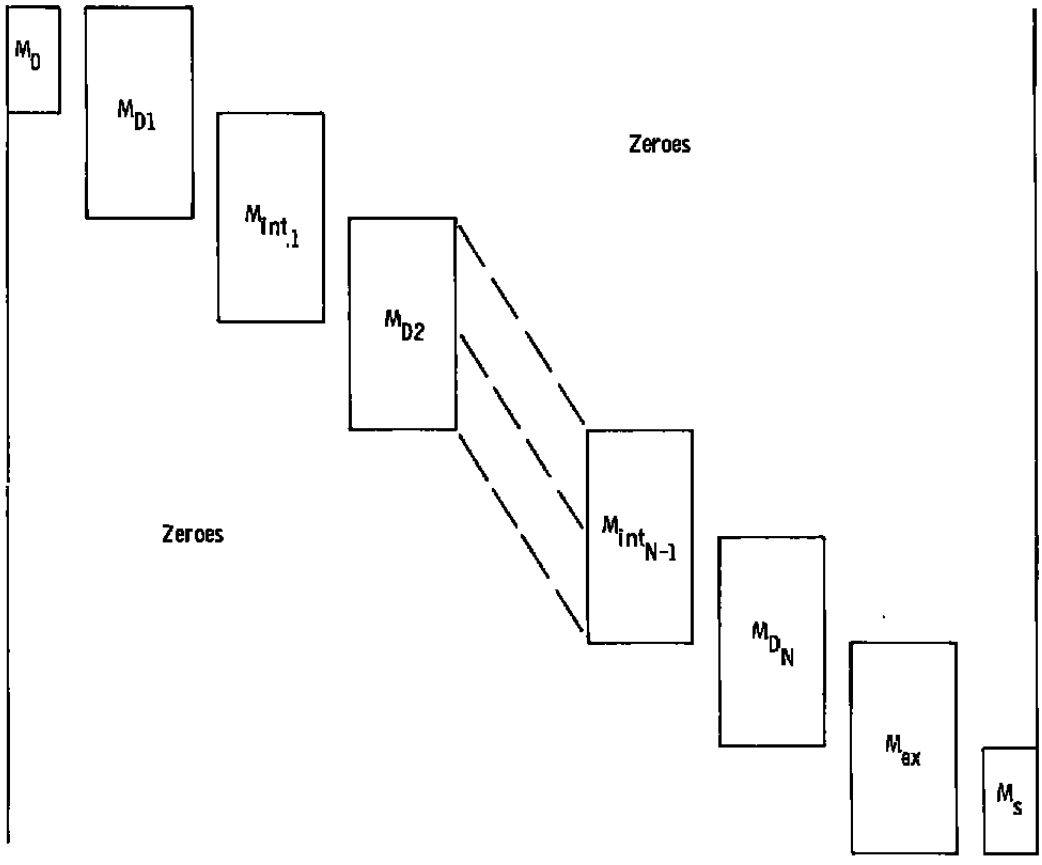

Figure 4. Block form of N damper interface matrix for either TM or TE waves.

Note that the intervening medium is not required to be free space but only nondissipative. The submatrices for TE waves are stated below:

$$M_o^M = \begin{pmatrix} \beta_{D_1} \frac{\mu}{\mu_{D_1}} \psi_\ell(a_o) \\ \psi_\ell'(a_o) \end{pmatrix} \tag{85a}$$

$$M_{D_j}^M = \begin{pmatrix} -\zeta_\ell^1\left(\beta_{D_j} a_{2j-2}\right) - \zeta_\ell^2\left(\beta_{D_j} a_{2j-2}\right) \\ -\zeta_\ell^{1'}\left(\beta_{D_j} a_{2j-2}\right) - \zeta_\ell^{2'}\left(\beta_{D_j} a_{2j-2}\right) \\ \zeta_\ell^1\left(\beta_{D_j} a_{2j-1}\right) \quad \zeta_\ell^2\left(\beta_{D_j} a_{2j-1}\right) \\ \zeta_\ell^{1'}\left(\beta_{D_j} a_{2j-1}\right) \quad \zeta_\ell^{2'}\left(\beta_{D_j} a_{2j-1}\right) \end{pmatrix} \tag{85b}$$

$$M_{int_j}^M = \begin{pmatrix} -\beta_{D_j} \frac{\mu}{\mu_{D_j}} \zeta_\ell^1\left(a_{2j-1}\right) & -\beta_{D_j} \frac{\mu}{\mu_{D_j}} \zeta_\ell^2\left(a_{2j-1}\right) \\ -\zeta_\ell^{1'}\left(a_{2j-1}\right) & -\zeta_\ell^{2'}\left(a_{2j-1}\right) \\ \beta_{D_{j+1}} \frac{\mu}{\mu_{D_{j+1}}} \zeta_\ell^1\left(a_{2j}\right) & \beta_{D_{j+1}} \frac{\mu}{\mu_{D_{j+1}}} \zeta_\ell^2\left(a_{2j}\right) \\ \zeta_\ell^{1'}\left(a_{2j}\right) & \zeta_\ell^{2'}\left(a_{2j}\right) \end{pmatrix} \tag{85c}$$

$$M_{ex}^M = \begin{pmatrix} -\beta_{D_N} \frac{\mu}{\mu_{D_N}} \zeta_\ell^1\left(a_{2N}\right) & -\beta_{D_N} \frac{\mu}{\mu_{D_N}} \psi_\ell\left(a_{2N}\right) \\ -\zeta_\ell^{2'}\left(a_{2N}\right) & -\psi_\ell'\left(a_{2N}\right) \\ \beta_s \frac{\mu}{\mu_s} \zeta_\ell^2\left(a_{2N+1}\right) & \beta_s \frac{\mu}{\mu_s} \psi_\ell\left(a_{2N+1}\right) \\ \zeta_\ell^{2'}\left(a_{2N+1}\right) & \psi_\ell'\left(a_{2N+1}\right) \end{pmatrix} \tag{85d}$$

$$M_S^M = \begin{pmatrix} -\zeta_\ell^1\left(\beta_s a_{2N+1}\right) \\ -\zeta^{1'}\left(\beta_s a_{2N+1}\right) \end{pmatrix} \tag{85e}$$

The modular nature of the interface matrices $\underline{M}^E$ and $\underline{M}^M$ is clearly demonstrated in Fig. 4. An empty cavity is represented by the submatrices M_o, M_{ex}, and M_s. For one damper the interface matrices are built up from M_o, M_{D_1}, M_{ex}, and M_s. A cavity containing two dampers is represented by the combination M_o, M_{D_1}, M_{int_1}, M_{ex}, and M_s. A three-damper cavity is represented by M_o, M_{D_1}, M_{int_1}, M_{D_2}, M_{int_2}, M_{D_3}, M_{ex}, and M_s, etc. Thus a damper can be added to or subtracted from the computational scheme merely by adding or subtracting a damper submatrix M_{D_j} and a submatrix M_{int_j}, corresponding to the intermediate region between the "j*th*" damper and the "j + 1*th*" damper.

In practice, the surface conductivity is sufficiently high that the asymptotic approximations,

$$\zeta_\ell^{1'}(\beta_s a_s) \cong i\zeta_\ell^1(\beta_s a_s)$$

and

$$\zeta_\ell^1(\beta_s a_s) \cong e^{i[k_s a - \pi/2(\ell+1)]} \quad [\text{with } k_s = (1 + i)/(\delta_s)]$$

can be used to simplify the corresponding elements in Eqs. (84e) and (85e). No such simplification can be applied to the remaining matrix elements, since $\alpha_s = 2.74$ corresponds to the primary TM mode of any spherical cavity. Nevertheless, these matrix elements can be stably computed by using standard, downward recursion algorithms with less memory requirement than the current AEDC Mie-scattering codes require.

It is apparent that the interface matrices are sparse, tetra-diagonal matrices. While the innermost two diagonals contain exclusively nonzero elements, the outermost two contain alternating zero and nonzero elements. This structure can be used advantageously to devise efficient inversion algorithms to solve Eq. (81).

There are three significant advantages to using a matrix approach to solve the boundary value problem instead of using the direct solutions presented in the next section: (1) Because of the modular nature of the matrix, the number of dampers considered can be altered by merely adding or deleting blocks in the interface matrix, as explained earlier. (2) Less computational difficulty (and less program complexity) should result from computing the spherical functions used in Eqs. (84) and (85) (once, for each frequency of interest) and numerically inverting Eq. (82) to obtain the desired multipole coefficients (instead of using the complicated combinations of these functions appearing in the next section). (3) If only

the frequency response of the source-cavity system (hence, the frequency dependence of the antenna impedance) is desired, rather than the electric and magnetic field distributions in the cavity, then only the standing wave coefficients A_ℓ^m and B_ℓ^m need be computed. (Only A_ℓ^o need be computed for an axisymmetric source.) The direct solution procedure, in effect, requires that all other multipole coefficients be computed in the process of determination of A_ℓ^m and B_ℓ^m. Of course the matrix procedure is capable of simultaneously determining all other multipole coefficients, but they need not be computed, unless desired.

3.3.2.1 Multipole Coefficients for a Cavity Containing a Single Damper

To illustrate the direct solution procedure, let us solve the single damper problem explicitly. The equations that relate the interior, damped, and exterior solutions are analogous to Eq. (75) and are stated below for TM waves:

$$\beta_D \frac{\epsilon}{\bar{\epsilon}_D}\left[a_\ell^m \zeta_\ell^1(a_o) + A_\ell^m \psi_\ell(a_o)\right] = {}^{+}a_{1,\ell}^m \zeta_\ell^1\left(\beta_D a_o\right) + {}^{-}a_{1,\ell}^m \zeta_\ell^2\left(\beta_D a_o\right)$$

$$\beta_D^2 \frac{\epsilon}{\bar{\epsilon}_D}\frac{\mu}{\mu_D}\left[a_\ell^m \zeta_\ell^{1'}(a_o) + A_\ell^m \psi_\ell'(a_o)\right] = {}^{+}a_{1,\ell}^m \zeta_\ell^{1'}\left(\beta_D a_o\right) + {}^{-}a_{1,\ell}^m \zeta_\ell^{2'}\left(\beta_D a_o\right)$$

$$\frac{\bar{\epsilon}_D}{\beta_D \epsilon}\left[{}^{+}a_\ell^m \zeta_\ell^1\left(\beta_D a_1\right) + {}^{-}a_\ell^m \zeta_\ell^2\left(\beta_D a_1\right)\right] = {}^{-}e_\ell^m \zeta_\ell^2(a_1) + E_\ell^m \psi_\ell(a_1)$$

$$\frac{\bar{\epsilon}_D \mu_D}{\beta_D^2 \epsilon \mu}\left[{}^{+}a_\ell^m \zeta_\ell^{1'}\beta_D a_1 + {}^{-}a_\ell^m \zeta_\ell^{2'}\left(\beta_D a_1\right)\right] = {}^{-}e_\ell^m \zeta_\ell^{2'}(a_1) + E_\ell^m \psi_\ell'(a_1)$$

$$\beta_s \frac{\epsilon}{\bar{\epsilon}_s}\left[e_\ell^m \zeta_\ell^2(a_s) + E_\ell^m \psi_\ell(a_s)\right] = {}^{+}\gamma_\ell^m \zeta_\ell^1\left(\beta_s a_s\right)$$

$$\beta_s^2 \frac{\epsilon}{\bar{\epsilon}_s}\frac{\mu}{\mu_s}\left[e_\ell^m \zeta_\ell^{2'}(a_s) + E_\ell^m \psi_\ell'(a_s)\right] = {}^{+}\gamma_\ell^m \zeta_\ell^{1'}\left(\beta_s a_s\right) \qquad (86)$$

The simplest way to solve these equations is to work backward from the surface, obtaining each TM wave multipole coefficient in terms of the coefficient in the immediately exterior, adjacent region. This very cumbersome procedure yields the following equations [using the asymptotic forms of $\zeta_\ell^1(\beta_s a_s)$ and $\zeta_\ell^{1'}(\beta_s a_s)$]:

$$y_\ell^m = \frac{2\,i\,a_\ell^m\,\beta_D\,\frac{\mu}{\mu_D}\,e^{-i\left[k_s R - \frac{\pi}{2}(\ell+1)\right]}}{\left[i\,\psi_\ell(a_s) - \beta_s\,\frac{\mu}{\mu_s}\,\psi_\ell'(a_s)\right]\left[\beta_D\,\frac{\mu}{\mu_D}\,D_{III}\,\zeta_\ell^2\left(\beta_D\,a_1\right) - C_{III}\,\zeta_\ell^{2\prime}\left(\beta_D\,a_1\right)\right]} \tag{87a}$$

$$e_\ell^m = \frac{-2\,\beta_D\,\frac{\mu}{\mu_D}\,a_\ell^m}{\beta_D\,\frac{\mu}{\mu_D}\,D_{III}\,\zeta_\ell^2(a_1) - C_{III}\,\zeta_\ell^{2\prime}\left(\beta_D\,a_1\right)} \tag{87b}$$

$$E_\ell^m = \frac{2\,\beta_D\,\frac{\mu}{\mu_D}\,a_\ell^m\left[\beta_s\,\frac{\mu}{\mu_s}\,\zeta_\ell^{2\prime}(a_s) - i\,\zeta_\ell^2(a_s)\right]}{\left[\beta_D\,\frac{\mu}{\mu_D}\,D_{III}\,\zeta_\ell^2\left(\beta_D\,a_1\right) - C_{III}\,\zeta_\ell^{2\prime}\left(\beta_D\,a_1\right)\right]\left[\beta_s\,\frac{\mu}{\mu_s}\,\psi_\ell'(a_s) - i\,\psi_\ell(a_s)\right]} \tag{87c}$$

$${}^{+}a_{1,\ell}^m = \frac{i\,a_\ell^m}{D_{II}\,\psi_\ell(a_o) - \beta_D\,\frac{\mu}{\mu_D}\,C_{II}\,\psi_\ell'(a_o)} \tag{87d}$$

$${}^{-}a_{1,\ell}^m = \frac{-i\,a_\ell^m\left[\beta_D\,\frac{\mu}{\mu_D}\,D_{III}\,\zeta_\ell^1\left(\beta_D\,a_1\right) - C_{III}\,\zeta_\ell^{1\prime}\left(\beta_D\,a_1\right)\right]}{\left[D_{II}\,\psi_\ell(a_o) - \beta_D\,\frac{\mu}{\mu_D}\,C_{II}\,\psi_\ell'(a_o)\right]\left[\beta_D\,\frac{\mu}{\mu_D}\,D_{III}\,\zeta_\ell^2\left(\beta_D\,a_1\right) - C_{III}\,\zeta_\ell^{2\prime}\left(\beta_D\,a_1\right)\right]} \tag{87e}$$

$$A_\ell^m = \frac{a_\ell^m\left[\beta_D\,\frac{\mu}{\mu_D}\,C_{II}\,\zeta_\ell^{1\prime}(a_o) - D_{II}\,\zeta_\ell^{1\prime}(a_o)\right]}{\left[D_{II}\,\psi_\ell(a_o) - \beta_D\,\frac{\mu}{\mu_D}\,C_{II}\,\psi_\ell'(a_o)\right]} \tag{87f}$$

The coefficients with Roman subscripts in Eq. (87) are not constants but are the auxiliary functions stated below:

$$C_{III} = \frac{\beta_s\,\frac{\mu}{\mu_s}\left[\psi_\ell(a_1)\,\zeta_\ell^{2\prime}(a_s) - \psi_\ell'(a_s)\,\zeta_\ell^2(a_1)\right] - i\left[\psi_\ell(a_1)\,\zeta_\ell^2(a_s) - \zeta_\ell^2(a_1)\,\psi_\ell(a_s)\right]}{i\,\psi_\ell(a_s) - \beta_s\,\frac{\mu}{\mu_s}\,\psi_\ell'(a_s)}$$

$$D_{III} = \frac{\partial\,C_{III}}{\partial a_1}$$

$$C_{II} = \frac{C_{III}\left\{\left[\zeta_\ell^2\left(\beta_D a_o\right)\zeta_\ell^{1\prime}\left(\beta_D a_1\right) - \zeta_\ell^{2\prime}\left(\beta_D a_1\right)\zeta_\ell^1\left(\beta_D a_o\right)\right]\right.}{\left.- \beta_D \frac{\mu}{\mu_D} D_{III}\left[\zeta_\ell^1\left(\beta_D a_1\right)\zeta_\ell^2\left(\beta_D a_o\right) - \zeta_\ell^1\left(\beta_D a_o\right)\zeta_\ell^2\left(\beta_D a_1\right)\right]\right\}}{\left[\beta_D \frac{\mu}{\mu_D} D_{III}\,\zeta_\ell^2\ \beta_D a_1\ - C_{III}\,\zeta_\ell^{2\prime}\left(\beta_D a_1\right)\right]}$$

$$D_{II} = \frac{\partial C_{II}}{\partial \beta_D a_o} \tag{88}$$

(Note that the Roman subscripts correspond to regions in Fig. 3.) The inconvenience of using these direct solutions, in contrast to the apparent simplicity of the numerical inversion procedure advocated in the previous section, is annoyingly obvious!

The TE wave multipole coefficients for the single-damper configuration are obtained in a similar fashion and are stated below:

$${}^{+}\delta_\ell^m = \frac{2\,i\,b_\ell^m\,\beta_s\,\beta_D\,\frac{\mu^2}{\mu_s\,\mu_D}\,e^{-i\left[k_s R - \frac{\pi}{2}(\ell+1)\right]}}{\left[\psi_\ell'(\alpha_s) - i\,\beta_s\,\frac{\mu}{\mu_s}\,\psi_\ell(\alpha_s)\right]\left[\varepsilon_{III}\,\zeta_\ell^2\left(\beta_D a_1\right) - \beta_D\,\frac{\mu}{\mu_D}\,f_{III}\,\zeta_\ell^{2\prime}\left(\beta_D a_1\right)\right]} \tag{89a}$$

$${}^{-}m_\ell^m = \frac{-2\,\beta_D\,\frac{\mu}{\mu_D}\,b_\ell^m}{\varepsilon_{III}\,\zeta_\ell^2\left(\beta_D a_1\right) - \beta_D\,\frac{\mu}{\mu_D}\,f_{III}\,\zeta_\ell^{2\prime}\left(\beta_D a_1\right)} \tag{89b}$$

$$M_\ell^m = \frac{2\,\beta_D\,\frac{\mu}{\mu_D}\,b_\ell^m\left[i\,\beta_s\,\frac{\mu}{\mu_s}\,\zeta_\ell^2(a_s) - \zeta_\ell^{2\prime}(a_s)\right]}{\left[\varepsilon_{III}\,\zeta_\ell^2\left(\beta_D a_1\right) - \beta_D\,\frac{\mu}{\mu_D}\,f_{III}\,\zeta_\ell^{2\prime}\left(\beta_D a_1\right)\right]\left[i\,\beta_s\,\frac{\mu}{\mu_s}\,\psi_\ell(a_s) - \psi_\ell'(a_s)\right]} \tag{89c}$$

$${}^{+}\beta_{1,\ell}^m = \frac{i\,\beta_D\,\frac{\mu}{\mu_D}\,b_\ell^m}{\beta_D\,\frac{\mu}{\mu_D}\,\varepsilon_{II}\,\psi_\ell(a_o) - f_{II}\,\psi_\ell'(a_o)} \tag{89d}$$

$$-\beta^{m}_{1,\ell} = \frac{-\,i\,\beta_D\,\frac{\mu}{\mu_D}\,b^{m}_{\ell}\left[\,g_{III}\,\zeta^{1}_{\ell}\left(\beta_D\,a_1\right) - f_{III}\,\beta_D\,\frac{\mu}{\mu_D}\,\zeta^{1}_{\ell}{}'\left(\beta_D\,a_1\right)\right]}{\left[\beta_D\,\frac{\mu}{\mu_D}\,g_{II}\,\psi_{\ell}\left(a_o\right) - f_{II}\,\psi'_{\ell}\left(a_o\right)\right]\left[\,g_{III}\,\zeta^{2}_{\ell}\left(\beta_D\,a_1\right) - \beta_D\,\frac{\mu}{\mu_D}\,f_{III}\,\zeta^{2}_{\ell}{}'\left(\beta_D\,a_1\right)\right]} \tag{89e}$$

$$B^{m}_{\ell} = b^{m}_{\ell}\left[\frac{\beta_D\,\frac{\mu}{\mu_D}\,g_{II}\,\zeta^{1}_{\ell}\left(a_o\right) - f_{II}\,\zeta^{1}_{\ell}{}'\left(a_o\right)}{f_{II}\,\psi'_{\ell}\left(a_o\right) - \beta_D\,\frac{\mu}{\mu_D}\,g_{II}\,\psi_{\ell}\left(a_o\right)}\right] \tag{89f}$$

The associated auxiliary functions are the following:

$$f_{III} = \frac{i\,\beta_a\,\frac{\mu}{\mu_a}\left[\zeta^{2}_{\ell}(a_1)\;\psi_{\ell}\left(a_a\right) - \psi_{\ell}\left(a_1\right)\,\zeta^{2}_{\ell}\left(a_a\right)\right] - \left[\zeta^{2}_{\ell}(a_1)\;\psi_{\ell}{}'\left(a_a\right) - \psi_{\ell}\left(a_1\right)\,\zeta^{2}_{\ell}{}'\left(a_a\right)\right]}{i\,\beta_a\,\frac{\mu}{\mu_a}\;\psi_{\ell}\left(a_a\right) - \psi'_{\ell}\left(a_a\right)}$$

$$g_{III} = \frac{\partial f_{III}}{\partial a_1}$$

$$f_{II} = \frac{g_{III}\left\{\left[\zeta^{1}_{\ell}\left(\beta_D\,a_o\right)\zeta^{2}_{\ell}\left(\beta_D\,a_1\right) - \zeta^{1}_{\ell}\left(\beta_D\,a_1\right)\zeta^{2}_{\ell}\left(\beta_D\,a_o\right)\right]\right.}{\left.-\,\beta_D\,\frac{\mu}{\mu_D}\;f_{III}\left[\zeta^{1}_{\ell}\left(\beta_D\,a_o\right)\zeta^{2}{}'_{\ell}\left(\beta_D\,a_1\right) - \zeta^{1}{}'_{\ell}\left(\beta_D\,a_1\right)\zeta^{2}_{\ell}\left(\beta_D\,a_o\right)\right]\right\}}{\left[g_{III}\,\zeta^{2}_{\ell}\left(\beta_D\,a_1\right) - \beta_D\,\frac{\mu}{\mu_D}\,f_{III}\,\zeta^{2}_{\ell}{}'\left(\beta_D\,a_1\right)\right]}$$

$$g_{II} = \frac{\partial f_{II}}{\partial \beta_D\,a_o} \tag{90}$$

Since most treatments of damping grids assume that the grids are infinitely thin surfaces across which the tangential magnetic field is discontinuous (with this discontinuity proportional to the surface current), it is important to determine *when* the finite width of the dampers must be considered. Let the damper width be $D = r_b - r_a$. Now, simplified shifted argument expansions of the Ricatti-Hänkel functions and their derivatives can be stated (Ref. 5) as

$$\zeta^{1,2}_{\ell}\left(\beta_D\,a_o\right) \simeq \zeta^{1,2}_{\ell}\left(\beta_D\,a_1\right) - \beta_D\,a_D\;\zeta^{1,2}{}'\;\beta_D\,a_1$$

$$\zeta^{1,2}{}'_{\ell}\left(\beta_D\,a_o\right) \simeq \zeta^{1,2}{}'_{\ell}\left(\beta_D\,a_1\right) - \frac{\beta_D\,a_D}{2}\left[\frac{\ell(\ell+1)}{\left(\beta_D\,a_1\right)^2} - 1\right]\zeta^{1,2}_{\ell}\left(\beta_D\,a_1\right) \tag{91}$$

where $\alpha_D = \alpha_1 - \alpha_o = kD$, and analogous relations can be derived for the Ricatti-Bessel functions. Equation (91) relates the damped spherical waves at the inner damper radius to those at the outer damper radius. After some manipulation involving the Wronkskian, $W[\zeta_\ell^1(\beta_D\alpha_1), \zeta_\ell^2(\beta_D\alpha_1)]$ (see Ref. 5), we find that, in order to ignore the finite width of the damper in the computation of C_{II} and D_{II}, the following inequalities must be simultaneously satisfied:

$$\left|\beta_D^2 \frac{\mu}{\mu_D} \alpha_D\right| << \left|\frac{C_{III}}{D_{III}}\right| \text{ and } \frac{\mu_D}{\mu} \alpha_D \left|\frac{\ell(\ell+1)}{(\beta_D \alpha_1)^2} - 1\right| << \left|\frac{D_{III}}{C_{III}}\right|$$

Thus,

$$(k_D D)^2 = (\beta_D \alpha_D)^2 << \left|\frac{\ell(\ell+1)}{(\beta_D \alpha_1)^2} - 1\right|^{-1} \tag{92}$$

For the lower-order multipoles, Eq. (92) simply states that the finite width of the damper can be ignored if it is much less than $\lambda_D/2\pi$ where λ_D is the wavelength of the TM wave in the damper. The higher-order ($\ell > 1$) multipoles, however, contribute to the high frequency response of the system because Bessel functions peak at values of their arguments which are comparable to their order. To understand the significance of Eq. (92), we consider a case where the damper impedance is $1/\sqrt{2}$ times that of the intervening medium and the damper is located at half the chamber radius: Then, $\alpha_1 = 0.7\,\alpha_{s\,\ell,j}$, where $\psi_\ell'(\alpha_{s\,\ell,j}) = 0$ corresponds to the TM eigenmode of *ℓth* order and *jth* degeneracy. Consider the case of $\ell = 3$, since even-order multipoles vanish for a source with axisymmetry. Then, $\alpha_{s\,3,1} \cong 1.5\,\alpha_{s\,1,1}$; thus, Eq. (92) becomes

$$D^2 << \left(\frac{\lambda_D}{2\pi}\right)^2 \left(\frac{12}{(1.3)^2} - 1\right)^{-1/2} \text{ or } D << 0.4\,\frac{\lambda_D}{2\pi}$$

The finite width of the damper is more significant when the chamber resonance is of a high order and the damper is near the center of the chamber.

If desired, the preceding Eqs. (86) through (89) can be simplified by retention of only first-order terms in the damper width. The auxiliary functions, C_{II} and D_{II}, reduce to

$$C_{II} = 2i\left[\frac{C_{III} - \beta^2 \frac{\mu}{\mu_D} \alpha_D D_{III}}{\beta_D \frac{\mu}{\mu_D} D_{III} \zeta_\ell^2(\beta_D \alpha_1) - C_{III} \zeta_\ell^{2\prime}(\beta_D \alpha_1)}\right]$$

$$D_{II} = 2i\left[\frac{\beta_D \frac{\mu}{\mu_D} D_{III} - \beta_D \alpha \quad C_{III}\left(\frac{\ell(\ell+1)}{\alpha_1^2} - 1\right)}{\beta_D \frac{\mu}{\mu_D} D_{III} \zeta_\ell^2(\beta_D \alpha_1) - C_{III} \zeta_\ell^{2\prime}(\beta \quad \alpha_1)}\right] \tag{88a}$$

with similar reductions for f_{II} and g_{II}. Equations (87d) through (87f) are then evaluated with α_0 replaced by α_I and using Eq. (88a) for C_{II} and D_{II}. Obviously, an analogous procedure can be applied to Eqs. (89d) through (89f).

Simplifications such as Eq. (91) can also be applied to the submatrices in Eqs. (84) and (85). These approximations offer the obvious advantage of reducing the number of spherical functions to be computed. In addition, they isolate the small parameter, α_D, in case special precautions must be taken in the inversion procedure to avoid loss of significant digits accuracy.

3.3.2.2 Multipole Coefficients for a Cavity Containing Two Dampers.

The TM wave multipole expansion coefficients (using the notation convention of Section 3.3) for the two-damper cavity in Fig. 5 are given below (assuming, for simplicity, that the electrical properties of both dampers are the same):

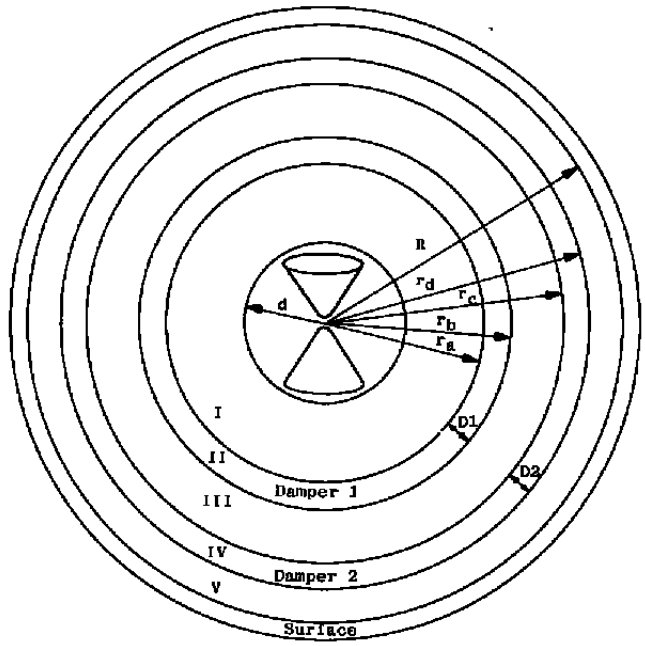

Figure 5. Geometry for electromagnetic wave propagation in an internally excited hollow sphere containing two concentric damping regions.

$$ {}^{+}y_{\ell}^{m} = \frac{8\,i\left(\beta_D \frac{\mu}{\mu_D}\right)^2 a_{\ell}^{m}\, e^{-i\left[k_s R - \frac{\pi}{2}(\ell+1)\right]}}{\left[\beta_s \frac{\mu}{\mu_s}\psi_{\ell}'(a_s) - i\psi_{\ell}(a_s)\right]\left[\beta_D \frac{\mu}{\mu_D} D_V \zeta_{\ell}^{2}\left(\beta_D a_3\right) - C_V \zeta_{\ell}^{2\prime}\left(\beta_D a_3\right)\right]\left[\beta_D \frac{\mu}{\mu_D} C_{IV}\zeta_{\ell}^{2\prime}(a_2) - D_{IV}\zeta_{\ell}^{2}(a_2)\right]\left[\beta_D \frac{\mu}{\mu_D} D_{III}\zeta_{\ell}^{2}\left(\beta_D a_1\right) - C_{III}\zeta_{\ell}^{2\prime}\left(\beta_D a_1\right)\right]\left[\beta_D \frac{\mu}{\mu_D} C_{II}\psi_{\ell}'(a_o) - D_{II}\psi_{\ell}(a_o)\right]} \tag{93a} $$

$$ {}^{-}c_{\ell}^{m} = \frac{8\left(\beta_D \frac{\mu}{\mu_D}\right)^2 a_{\ell}^{m}}{\left[\beta_D \frac{\mu}{\mu_D} D_V \zeta_{\ell}^{2}\left(\beta_D a_3\right) - C_V \zeta_{\ell}^{2\prime}\left(\beta_D a_3\right)\right]\left[\beta_D \frac{\mu}{\mu_D} C_{IV}\zeta_{\ell}^{2\prime}(a_2) - D_{IV}\zeta_{\ell}^{2}(a_2)\right]\left[\beta_D \frac{\mu}{\mu_D} D_{III}\zeta_{\ell}^{2}\left(\beta_D a_1\right) - C_{III}\zeta_{\ell}^{2\prime}\left(\beta_D a_1\right)\right]\left[\beta_D \frac{\mu}{\mu_D} C_{II}\psi_{\ell}'(a_o) - D_{II}\psi_{\ell}(a_o)\right]} \tag{93b} $$

$$ E_{\ell}^{m} = \frac{-8\left(\beta_D \frac{\mu}{\mu_D}\right)^2 a_{\ell}^{m}\left[\beta_s \frac{\mu}{\mu_s}\zeta_{\ell}^{2\prime}(a_s) - i\,\zeta_{\ell}^{2}(a_s)\right]}{\left[\beta_s \frac{\mu}{\mu_s}\psi_{\ell}'(a_s) - i\psi_{\ell}(a_s)\right]\left[\beta_D \frac{\mu}{\mu_D} D_V \zeta_{\ell}^{2}\left(\beta_D a_3\right) - C_V \zeta_{\ell}^{2}\left(\beta_D a_3\right)\right]\left[\beta_D \frac{\mu}{\mu_D} C_{IV}\zeta_{\ell}^{2\prime}(a_2) - D_{IV}\zeta_{\ell}^{2}(a_2)\right]\left[\beta_D \frac{\mu}{\mu_D} D_{III}\zeta_{\ell}^{2}\left(\beta_D a_1\right) - C_{III}\zeta_{\ell}^{2\prime}\left(\beta_D a_1\right)\right]\left[\beta_D \frac{\mu}{\mu_D} C_{II}\psi_{\ell}'(a_o) - D_{II}\psi_{\ell}(a_o)\right]} \tag{93c} $$

$$ {}^{+}a_{2,\ell}^{m} = \frac{-4\,i\left(\beta_D \frac{\mu}{\mu_D}\right) a_{\ell}^{m}}{\left[\beta_D \frac{\mu}{\mu_D} C_{IV}\zeta_{\ell}^{2\prime}(a_2) - D_{IV}\zeta_{\ell}^{2}(a_2)\right]\left[\beta_D \frac{\mu}{\mu_D} D_{III}\zeta_{\ell}^{2}\left(\beta_D a_1\right) - C_{III}\zeta_{\ell}^{2\prime}\left(\beta_D a_1\right)\right]\left[\beta_D \frac{\mu}{\mu_D} C_{II}\psi_{\ell}'(a_o) - D_{II}\psi_{\ell}(a_o)\right]} \tag{93d} $$

$$ {}^{-}a_{2,\ell}^{m} = \frac{4\,i\left(\beta_D \frac{\mu}{\mu_D}\right) a_{\ell}^{m}\left[\beta_D \frac{\mu}{\mu_D} D_V \zeta_{\ell}^{1}\left(\beta_D a_3\right) - C_V \zeta_{\ell}^{1\prime}\left(\beta_D a_3\right)\right]}{\left[\beta_D \frac{\mu}{\mu_D} D_V \zeta_{\ell}^{2}\left(\beta_D a_3\right) - C_V \zeta_{\ell}^{2\prime}\left(\beta_D a_3\right)\right]\left[\beta_D \frac{\mu}{\mu_D} C_{IV}\zeta_{\ell}^{2\prime}(a_2) - D_{IV}\zeta_{\ell}^{2}(a_2)\right]\left[\beta_D \frac{\mu}{\mu_D} D_{III}\zeta_{\ell}^{2}\left(\beta_D a_1\right) - C_{III}\zeta_{\ell}^{2\prime}\left(\beta_D a_1\right)\right]\left[\beta_D \frac{\mu}{\mu_D} C_{II}\psi_{\ell}'(a_o) - D_{II}\psi_{\ell}(a_o)\right]} \tag{93e} $$

$$ {}^{+}C_{1,\ell}^{m} = \frac{2\left(\beta_D \frac{\mu}{\mu_D}\right) a_{\ell}^{m}}{\left[\beta_D \frac{\mu}{\mu_D} D_{III}\zeta_{\ell}^{2}\left(\beta_D a_1\right) - C_{III}\zeta_{\ell}^{2\prime}\left(\beta_D a_1\right)\right]\left[\beta_D \frac{\mu}{\mu_D}\psi_{\ell}'(a_o) - D_{II}\psi_{\ell}(a_o)\right]} \tag{93f} $$

$$ {}^{-}C_{1,\ell}^{m} = \frac{-2\left(\beta_D \frac{\mu}{\mu_D}\right) a_{\ell}^{m}\left[\beta_D \frac{\mu}{\mu_D} C_{IV}\zeta_{\ell}^{1\prime}(a_2) - D_{IV}\zeta_{\ell}^{1}(a_2)\right]}{\left[\beta_D \frac{\mu}{\mu_D} C_{IV}\zeta_{\ell}^{2\prime}(a_2) - D_{IV}\zeta_{\ell}^{2}(a_2)\right]\left[\beta_D \frac{\mu}{\mu_D} D_{III}\zeta_{\ell}^{2}\left(\beta_D a_1\right) - C_{III}\zeta_{\ell}^{2\prime}\left(\beta_D a_1\right)\right]\left[\beta_D \frac{\mu}{\mu_D} C_{II}\psi_{\ell}'(a_o) - D_{II}\psi_{\ell}(a_o)\right]} \tag{93g} $$

$$ {}^{+}a_{1,\ell}^{m} = \frac{i\,a_{\ell}^{m}}{\left[\beta_D \frac{\mu}{\mu_D} C_{II}\psi_{\ell}'(a_o) - D_{II}\psi_{\ell}(a_o)\right]} \tag{93h} $$

In these equations, ${}^{+}\gamma_\ell^m$ are the multipole coefficients of outward propagating waves at the inner radius of the sphere surface; e_ℓ^m, inward propagating waves at the inner surface of the sphere; E_ℓ^m, standing waves between the outer damper and the sphere inner surface; ${}^{\pm}\alpha_{2,\ell}^m$, outward and inward propagating waves, respectively, in the outer damper; ${}^{\pm}C_{1\ell}^m$, outward and inward propagating waves, respectively, in the region between the two dampers; ${}^{+}\alpha_{1,\ell}^m$, outward and inward propagating waves, respectively, in the inner damper; and A_ℓ^m, standing waves between the inner damper and the center of the sphere (exclusive of the source).

$$-\alpha_{1,\ell}^m = -\frac{i\, a_\ell^m \left[\beta_D \frac{\mu}{\mu_D} D_{III}\, \zeta_\ell^1(\beta_D a_1) - C_{III}\, \zeta_\ell^{1\prime}(\beta_D a_1)\right]}{\left[\beta_D \frac{\mu}{\mu_D} D_{III}\, \zeta_\ell^2(\beta_D a_1) - C_{III}\, \zeta_\ell^{2\prime}(\beta_D a_1)\right]\left[\beta_D \frac{\mu}{\mu_D} C_{II}\, \psi_\ell'(a_o) - D_{II}\, \psi_\ell(a_o)\right]} \tag{93i}$$

$$A_\ell^m = -a_\ell^m \left[\frac{\beta_D \frac{\mu}{\mu_D} C_{II}\, \zeta_\ell^{1\prime}(a_o) - D_{II}\, \zeta_\ell^1(a_o)}{\beta_D \frac{\mu}{\mu_D} C_{II}\, \psi_\ell'(a_o) - D_{II}\, \psi_\ell(a_o)}\right] \tag{93j}$$

$$C_V = \frac{\beta_s \frac{\mu}{\mu_s}\left[\zeta_\ell^2(a_3)\,\psi_\ell'(a_s) - \psi_\ell(a_3)\,\zeta_\ell^{2\prime}(a_s)\right] - i\left[\zeta_\ell^2(a_3)\,\psi_\ell(a_s) - \psi_\ell(a_3)\,\zeta_\ell^{2}(a_s)\right]}{\beta_s \frac{\mu}{\mu_s}\psi_\ell'(a_s) - i\,\psi_\ell(a_s)}$$

$$D_V = \frac{\partial C_V}{\partial a_3}$$

$$C_{IV} = \frac{\beta_D \frac{\mu}{\mu_D} D_V\left[\zeta_\ell^1(\beta_D a_2)\,\zeta_\ell^2(\beta_D a_3) - \zeta_\ell^2(\beta_D a_2)\,\zeta_\ell^1(\beta_D a_3)\right] - C_V\left[\zeta_\ell^1(\beta_D a_3)\,\zeta_\ell^{2\prime}(\beta_D a_3) - \zeta_\ell^2(\beta_D a_3)\,\zeta_\ell^{1\prime}(\beta_D a_2)\right]}{\beta_D \frac{\mu}{\mu_D} D_V\,\zeta_\ell^2(\beta_D a_3) - C_V\,\zeta_\ell^{2\prime}(\beta_D a_3)}$$

$$D_{IV} = \frac{\partial C_{IV}}{\partial(\beta_D a_2)}$$

$$C_{III} = \frac{\beta_D \frac{\mu}{\mu_D} C_{IV}\left[\zeta_\ell^1(a_1)\,\zeta_\ell^{2\prime}(a_2) - \zeta_\ell^2(a_1)\zeta_\ell^{1\prime}(a_1)\right] - D_{IV}\left[\zeta_\ell^1(a_1)\,\zeta_\ell^2(a_2) - \zeta_\ell^2(a_1)\,\zeta_\ell^1(a_2)\right]}{\beta_D \frac{\mu}{\mu_D} C_{IV}\,\zeta_\ell^{2\prime}(a_2) - D_{IV}\,\zeta_\ell^2(a_2)}$$

$$D_{III} = \frac{\partial C_{III}}{\partial a_1}$$

$$C_{II} = \frac{\beta_D \frac{\mu}{\mu_D} D_{III}\left[\zeta_\ell^1(\beta_D a_o)\,\zeta_\ell^2(\beta_D a_1) - \zeta_\ell^2(\beta_D a_o)\,\zeta_\ell^1(\beta_D a_1)\right] - C_{III}\left[\zeta_\ell^1(\beta_D a_o)\,\zeta_\ell^{2\prime}(\beta_D a_1) - \zeta_\ell^2(\beta_D a_o)\,\zeta_\ell^{1\prime}(\beta_D a_1)\right]}{\beta_D \frac{\mu}{\mu_D} D_{III}\,\zeta_\ell^2(\beta_D a_1) - C_{III}\,\zeta_\ell^{2\prime}(\beta_D a_1)}$$

$$D_{II} = \frac{\partial C_{II}}{\partial(\beta_D a_1)} \tag{94}$$

There are, of course, analogous equations for the TE wave multipole coefficients and their associated auxiliary functions, but these will not be stated.

3.3.3 Coupling of the Damped Cavity and the Biconical Source

As shown in previous sections, the multipole coefficients of standing waves in the center of a damped cavity (cavity multipole coefficients) are related to the source multipole coefficients through equations that account for the electrical properties of all other regions of the sphere. Thus, to the extent that linear superposition is valid, it is possible to calculate the electric and magnetic fields in the vicinity of the antenna by merely adding together the contributions of the source multipoles and the cavity multipoles. Strictly speaking, however, the problem is *not* linear, since the presence of the cavity modifies the current distribution in the source. In the treatment of Sections 3.2.1 and 3.2.2 this interaction has been neglected in determining the source current distribution and the associated source multipole coefficients. Since the problem is virtually intractable if this interaction is included, the conditions for which the linear approximation is adequate should be ascertained.

Essentially the source cannot "see" the first damper until the leading edge of the transmitted pulse reflects from the damper inner surface and arrives, again, at the antenna. Thus, linearity is an adequate assumption for all times $t < (2r_a/C)$. Accordingly, the linear treatment is valid for all circular frequencies, $\omega > (C/2r_a)$. This means that the theory is correct for reduced damper radii, $kr_\alpha > 1/2$, or reduced cavity radii (i.e., sphere "size parameters" in optical terminology), $kR > R/2r_a$). Since the primary TM resonant mode of the cavity occurs at $kR = 2.74$, linear coupling is valid as long as $r_a/R > (1/5.48) = 0.182$, and this limit has, indeed, not been violated in the VKF 12-ft sphere experiments in which $r_a/R = 0.8$. Obviously, the above limit must not be disregarded in experimental design, since the presence of any conducting surface as close as R/5.48 to the source will modify the source current distribution (at frequencies of interest) in comparison to the current distribution calculated when it is assumed that the source radiates into an unbounded medium.

Assuming the validity of linear superposition, and evaluating Eq. (17), we determine the impedance of the biconical source plus damped cavity to be

$$\tilde{Z}_A = i\frac{\tilde{Z}}{\pi \sin\theta_c}\left\{\frac{\Sigma_\ell (2\ell+1)^{1/2}\, P_\ell(\cos\theta_c)\left[a_\ell \zeta_\ell^{1\prime}(k\delta) + A_\ell \psi_\ell^{\prime}(k\delta)\right]}{\Sigma_\ell (2\ell+1)^{1/2}\, P_\ell^1(\cos\theta_c)\left[a_\ell \zeta_\ell^1(k\delta) + A_\ell \psi_\ell(k\delta)\right]}\right\} \quad (95)$$

where $A_\ell = A_\ell^o$, and it should be recalled that only odd values of ℓ contribute to the sums in Eq. (95), on account of the cylindrical symmetry of the biconical source. The frequency response of the system is, then, obtained by inserting Eq. (95) into Eq. (19) and evaluating (numerically) the results at all frequencies greater than $|\omega_{min}| = C/2r_a$.

4.0 RECOMMENDATIONS FOR FUTURE WORK AND CONCLUDING REMARKS

This report has presented a theoretical formulation to describe the propagation of both TM and TE waves through an internally excited, damped spherical cavity. The general treatment developed herein allows consideration of an arbitrary central source current distribution and an arbitrary number of dampers of finite width.

Several features of the present treatment are unique and worthy of further comment:

1. The present theory considers dampers with distributed electrical properties and finite width, and, if desired, each effective damper width can be treated as an adjustable parameter, in order to compensate for inhomogeneities in the damping mesh. Most similar investigations have assumed that the dampers can be treated as infinitely thin surfaces of discontinuity. While the finite damper width is not very significant in analysis of the 12-ft sphere experiments, some future analyses of damping configurations may require inclusion of finite width effects.

2. The present theory uses a matrix formulation to obtain the multipole expansion coefficients throughout the regions of a cavity containing N dampers. The computational flexibility afforded by the modular structure of this matrix permits easy addition or deletion of dampers. In addition, such an approach is computationally more convenient and probably more stable than more direct solution procedures. Although this matrix approach will be adopted in encoding the theory, explicit solutions for the single-damper and dual-damper multipole expansion coefficients are also presented in this report. In addition, the conditions under which the finite width of the dampers must be considered are investigated.

3. The present theory uses two scalar Hertz-Debye potentials to describe electric and magnetic fields outside the source region, whereas the conventional vector and scalar potentials are used by most authors There are two advantages associated with the use of these potentials:

a. The propagating fields are automatically separated into transverse magnetic (TM) and transverse electric (TE) waves in any geometry in which Laplace's equation is separable, and

b. The use of these potentials facilitates the solution of the inhomogeneous wave equations which represent the radiation from a centralized, arbitrary distribution of source currents. The Hertz-Debye potentials relate all other electric and magnetic field components to the radial field components, whose solutions are obtained by the use of Green's functions. These solutions show that only TM waves are radiated by cylindrically symmetric source currents, and TE waves are radiated either if an azimuthal current flow occurs or if azimuthal gradients in polar currents occur.

4. The present theory includes a closed-form solution for the multipole expansion coefficients which represent radiation into an unbounded medium by an uncapped biconical antenna. In addition, the two coupled integrodifferential equations—which separately describe the current distribution in the conical sections and in the caps of a capped biconical antenna, radiating into an unbounded medium—are derived by use of a gauge transformation. These equations can be solved by the method of moments or by a similar finite-element numerical technique. The multipole expansion coefficients for a capped bicone can then be obtained by substituting the bicone current expansion into the TM wave Green's function solution.

5. The frequency response (and, by inverse Fourier transformation, the time dependent pulse waveform) of the internally excited, damped cavity is obtained from the characteristic impedance of the bicone and the input impedance of the antenna, radiating into the damped cavity. This impedance, in turn, is calculated from the multipole expansion coefficients of the source and the first standing waves in the region between the source and the damper. The antenna impedance and frequency response of the antenna, radiating into an unbounded medium, can be obtained simply by setting the multipole coefficients of the standing waves equal to zero. This procedure provides a check on the accuracy of the source current solution.

Future work in this area should follow the directions indicated below:

1. Encode the theory, including the bicone source current determination, with options to calculate the (polar) angular and radial electric and magnetic field distributions throughout the cavity at specified frequencies and to calculate only the frequency response of the cavity at the bicone feed terminals (hence, by

inverse Fourier transformation, the wave form of the sensor current pulse). The primary result of this work would be a comparison between theory and experiment. The tasks that follow cannot be implemented until this has been accomplished.

2. Adapt the theory and its coding to cylindrical coordinates.

3. Account for the effect of openings to accommodate instrumentation and X-ray beam paths in the damping mesh. In an infinitely thin damper, such openings are denoted "Bethe appertures" when they are smaller than a wavelength, and they act as dipole sources located at the positions of the openings.

4. Generalize the theory to account for an off-centered, but still axisymmetric source.

REFERENCES

1. Jackson, J. D. *Classical Electrodynamics*. Second edition. Wiley, New York, 1975.

2. Stratton, J. A. *Electromagnetic Theory*. McGraw-Hill, New York, 1941.

3. Van Bladel, J. *Electromagnetic Fields*. McGraw-Hill, New York, 1964.

4. Gray, C. G. "Multipole Expansions of Electromagnetic Fields Using Debye Potentials." *American Journal of Physics*, Vol. 46, No. 2, February 1978, pp. 169-179.

5. Abramowitz, M. and Stegun, I. A., eds. *Handbook of Mathematical Functions with Formulas, Graphs, and Mathematical Tables*. U. S. Government Printing Office, Washington, D. C., 1964.

6. Shelkunoff, S. A. *Advanced Antenna Theory*. Wiley, New York, 1952.

7. Jones, D. S. *The Theory of Electromagnetism*. Pergamon Press, Oxford, 1964.

8. Harrington, R. F. *Field Computation by Moment Methods*. MacMillan, New York, 1968.

9. Butler, C. M. "Evaluation of Potential Integral at Singularity of Exact Kernel in Thin-Wire Calculations." *IEEE Transactions on Antennas and Propagation*, Vol. AP-23, 1975, pp. 293-295.

10. Wilton, D. R. and Butler, C. M. "Efficient Numerical Techniques for Solving Pocklington's Equation and Their Relationships to Other Methods." *IEEE Transactions on Antennas and Propagation*, Vol. AP-24, 1976, pp. 83-86.

11. Wilton, D. R. "Dynamic Analysis of a Loaded Conical Antenna Over a Ground Plane." AFOSR-TR-76-1080, August 1976.

12. Kantorovich, L. V. and Krylov, V. I. *Approximate Methods of Higher Analysis.* C. D. Benster, trans. Interscience Publishers, New York, 1958.

13. Butler, C. M. and Van Bladel, J. "Electromagnetic Fields in a Spherical Cavity Embedded in a Dissipative Medium." *IEEE Transactions on Antennas and Propagation*, Vol. AP-12, 1964, pp. 110-118.

NOMENCLATURE

A_ℓ^m	Standing TM wave multipole coefficients for central cavity region (exclusive of source)
a_ℓ^m	Source TM wave multipole coefficients
B	Magnetic induction
B_ℓ^m	Standing TE wave multipole coefficients for central cavity region (exclusive of source)
b_ℓ^m	Source TE wave multipole coefficients
$C_{II \cdot V}$	TM wave auxiliary functions defined in Eqs. (88) and (94)
c	Speed of light in vacuum
$\pm c_{j\ell}^m$	Outwardly and inwardly propagating TM wave multipole coefficients for region between "j*th*" and "j + 1*th*" dampers
D	Damper thickness
$\vec{D}$	Displacement
$D_{II \cdot V}$	Derivatives of TM wave auxiliary functions defined in Eqs. (88) and (94)
$\pm d_{j\ell}^m$	Outwardly and inwardly propagating TE wave multipole coefficients for region between "j*th* and "j + 1*th*" dampers
$\vec{E}$	Electric field
E_ℓ^m	Standing TM wave multipole coefficients for region between outermost damper and sphere surface
$\pm e_\ell^m$	Outwardly and inwardly propagating TM wave multipole coefficients for region between outermost damper and sphere surface
$f_{II, III}$	TE wave auxiliary functions defined in Eq. (90)

$G(r, r')$	Green's functions used in solution of inhomogeneous Helmholtz equations
$g_{II, III}$	Derivatives of TE wave auxiliary functions defined in Eq. (90)
H	Magnetic field
h	Axial length of single cone of a biconical antenna (see Fig. 2)
I	Electric current
$\tilde{I}_o$	Complex constant appearing in Eqs. (40) through (42)
$\vec{J}$	Electric current density
$J_{n,f}$	Integral defined in Eq. (45)
J_o	Source current density
$\mathcal{K}$	Kernel function defined in Eq. (71)
k	Wave propagation constant
k_o	Wave propagation constant for a nondissipative medium
L	Radial length of single cone of a biconical antenna (see Fig. 2)
$\vec{L} = -i\vec{r} \times \vec{\nabla}$	Angular momentum operator
$\mathfrak{L}(\vec{r}, n')$	Kernel function defined in Eq. (71)
$\underline{M}$	Interface matrices defined in Eqs. (84) and (85)
M_f^m	Standing TE wave multipole coefficients for region between outermost damper and sphere surface
$\bar{m}_f^m$	Inwardly propagating TE wave multipole coefficients for region between outermost damper and sphere surface
$\mathfrak{N}(\vec{r}, n')$	Kernel function defined in Eq. (71)

N	Number of dampers
$\vec{P}_{E,M}$	Hertz vectors defined by Eq. (19)
$P_\ell(\cos\theta)$	Legendre polynomial of order ℓ
R	Sphere radius
$R_{1,2}$	Distances defined in Eqs. (56) and (57)
$\vec{r}$	Position vector to field observation point
$\vec{r}'$	Position vector to source point
S	Scalar function defined in conjunction with Eq. (25)
s	Arbitrary scalar function
TE	Transverse electric
TM	Transverse magnetic
t	Time
t_{bc}	Thickness of current-carrying region in sides of antenna
t_{cp}	Thickness of current-carrying region in caps of antenna
$\vec{U}$	Transformed field defined in Eq. (49)
V	Potential difference between the two halves of a biconical antenna
$\vec{V}$	Arbitrary vector function
$\underline{X}$	Column vectors of unknown multipole coefficients [see Eq. (83)]
$\underline{Y}$	Column vectors associated with Eq. (83)
$Y_\ell^m(\theta,\phi)$	Spherical harmonic functions

Z	Wave impedance
Z_c	Characteristic impedance of a beconical antenna
Z_o	Impedance of a nondissipative medium
Z_{sp}	Impedance of free space
z	Coordinate along axis of symmetry
α_j	Dimensionless radius of the "j*th*" interface
$\pm\alpha_{jl'}^{m}$	Outwardly and inwardly propagating TM wave multipole coefficients at the "j*th*" interface
β	Ratio of propagation constants in dissipative and nondissipative media
$\pm\beta_{jl'}^{m}$	Outwardly and inwardly propagating TE wave multipole coefficients at the "j*th*" interface
$^{+}\gamma_{l'}^{m}$	Outwardly propagating TM wave multipole coefficients at the sphere surface
δ	Radial location of antenna tip (see Fig. 2)
δ_c	Penetration depth
$\delta_{l'}^{m}$	Outwardly propagating TE wave multipole coefficients at the sphere surface
ϵ	Real dielectric permittivity
$\bar{\epsilon}$	Complex dielectric permittivity
σ	Electrical conductivity
μ	Magnetic permeability
$\pi_{E,M}$	Hertz-Debye potentials for TM and TE waves

$\chi_\ell(k,k_a,d)$	Complementary antenna function defined in Eq. (48)
$\chi_{bc}^{1\pm}(\vec{r}, r', \phi')$ $\chi_{bc}^{2\pm}(\vec{r}, r', \phi')$ $\chi_{cp}^{1\pm}(r, \varrho, \phi')$ $\chi_{bc}^{1\pm}(\vec{r}, \varrho, \phi')$	Modified Green's functions defined in Eq. (64)
ϱ	Antenna cylindrical coordinate
ϱ_c	Charge density
ϱ_o	Radius of antenna cap
ψ	Gauge variable defined in Eq. (49)
$\psi_\ell(kr)$	Ricatti-Bessel functions of order ℓ
$\zeta_\ell^{1,2}(kr)$	Ricatti-Hänkel functions or order ℓ
λ	Wavelength
ω	Circular frequency

SUPERSCRIPTS

E	Pertains to electric Hertz-Debye potential (source of TM waves)
M	Pertains to magnetic Hertz-Debye potential (source of TE waves)
m	Azimuthal index for spherical expansion
T	Denotes matrix transpose
$'$	Denotes source coordinate (except in Sec. 3.3, where it denotes differentiation)
$\sim$	Denotes frequency domain
+	Denotes outwardly propagating wave

–	Denotes inwardly propagating wave
^	Denotes unit vector
→	Denotes vector

SUBSCRIPTS

A	Pertains to antenna
bc	Pertains to conical surfaces of biconical antenna
cp	Pertains to cap surfaces of biconical antenna
D	Pertains to damper
E	Pertains to electric Hertz-Debye potential (source of TM waves)
II, III, ...	Pertain to cavity regions shown in Figs. 3 and 5
ℓ	Polar index for spherical expansion
M	Pertains to magnetic Hertz-Debye potential (source of TE waves)
s	Denotes quantity evaluated at surface of cavity
‾	Denotes matrix or column vector